Technical Report

COPPER • BRASS • BRONZE

ON THE PHASES, MICROCONSTITUENTS AND MICROSTRUCTURES IN NICKEL-ALUMINUM BRONZES

A1310-XX/00
Copper Development Association Inc.

ON THE PHASES, MICROCONSTITUENTS AND MICROSTRUCTURES IN NICKEL-ALUMINUM BRONZES.

Paul R. Howell.

Department of Materials Science and Engineering.

The Pennsylvania State University, PA 16802.

Applied Research Laboratory,

State College PA 16804

CONTENTS.

ON THE PHASES, MICROCONSTITUENTS AND MICROSTRUCTURES IN NICKEL-ALUMINUM BRONZES.

1. Introduction.

The object of this review is to present a coherent picture of the nature, (and the nomenclature) of the phases, microconstituents and microstructures that develop in nickel-aluminum bronzes (NAB). The review is neither historical, nor is it exhaustive: rather, it is a critical appraisal of our current knowledge regarding fundamental aspects of the development of microstructures in NAB. The review begins with a brief description of the thermodynamics (phase diagrams), kinetics (TTT and CCT curves) and nature (microstructures developed) of the phase transformations that occur in binary Cu-Al binary alloys (Section 2). The proposed terminologies, which describe the phases that are present in both the binary Cu-Al and (quaternary) nickel-aluminum bronzes, are also introduced (Sections 2 and 3). This is deemed to be a necessary precursor to the section on microstrucural development (Section 4) in that the literature is replete with confusing (and sometimes incorrect) phase descriptions and identifications. The proposed terminology is based on the oft-ignored review by Brezina [1], several contemporary articles by Lorimer, Ridley and co-workers [2-9] and more recently by a trio of theses at Penn State by the author's students [10-12]. This terminology is put into perspective with respect to existing, but incomplete vertical sections of the Cu-Al-Ni-Fe phase diagrams (Section 3.4). In all cases however, the published phase diagrams have been re-drawn to reflect the proposed terminology.

The discussion on nomenclature includes the results of several key past studies by e.g., Cook et al., [13], Weill-Couly and Arnaud [14], Thomson and Edward [15], Culpan and Rose [16,17]. These studies are used to provide a coherent picture of the microstructures that are developed in NABs. The brief concluding discussion (Section 5),

is predicated on the results discussed with respect to both the binary Cu-Al system as detailed by the kinetic studies of Smith and Lindlief [18], Philip and Mack [19] (Section 2), and by Brezina [1] in the more complex nickel-aluminum bronzes (Section 3).

A rationale is provided for "predicting" which "microstructures" can be attained in NABs by judicious control of chemistry, cooling rate and tempering treatments.

2. The Aluminum-Copper Binary System.

2.1 Phases, Microconstituents and Terminology

In order to understand the complex phase relationships which exist in the quinternary NABs, it is first necessary to consider the binary Cu-Al system. Figure 1 presents the Cu-rich end of the Cu-Al phase diagram. This phase diagram is essentially that of Smith and Lindlief [18] but with δ (their terminology) replaced by γ_2 which is in more current usage. In reference [18], the eutectoid reaction was found to occur at 570°C ± 1°C and for a composition of 11.87%Al. Smith and Lindlief [18] also conducted a series of very careful isothermal transformation studies and a simplified and modified version of their resulting TTT curves is shown in Figure 2. At this juncture, Table 1 is introduced: it lists the phases/microconstituents which were identified in binary Cu-Al alloys by e.g., refs [18], [19] and [20] but with a modified (proposed) terminology that will be employed throughout the remainder of the review. The phases/microconstituents are described as follows:

α: *is the terminal fcc solid solution* and is observed in both the binary Cu-Al, and quarterary Al-Cu-Ni-Fe alloys. α is an equilibrium phase. A typical image of the α microconstituent is shown in Figure 3: a low magnification light micrograph of a slowly

cooled NAB*. The light etching phase is proeutectoid α, which precipitates as Widmanstatten rods in the high temperature β matrix. Figure 4 is a higher magnification image of a similar alloy; the co-existance of Widmanstatten α rods (light-etching) and pools of martensite, α_1', (dark etching) is illustrated.

β: *is the high temperature, secondary, b.c.c. solid solution;* β is formed in commercial NAB alloys as well as in the binary alloys. β is an equilibrium phase.

γ_2: *is an intermetallic phase*. It is an equilibrium phase in binary alloys: its presence in NAB alloys is deleterious and is generally avoided.

β_1: *is an ordered, transition phase*. It is based on the Cu_3Al crystal structure. Single phase 'beta one" has been reported in NAB [1], and the presence of discrete ordered intermediate phases, based on either Fe_3Al and/or NiAl have frequently been documented (and see section 3).

α_1': *is martensite*; the term α_1' is used "generically" even though Swan and Warlimont [20] showed that there are (at least) three different martensite polymorphs (Figure 5). The three polymorphs, designated α_1 (low aluminum), α_1' and α_1'' (high aluminum) were also described by Hasan et al. [5] in NAB. These latter authors produced α_1 by the simple expedient of quenching a Cu-9.4%Al-4.9%Ni-4.4%Fe alloy directly from the β phase field (i.e., by *supercritical annealing*). α_1' and α_1'' were generated in the same bronze by an *intercritical anneal* (i.e., in the two-phase $\alpha+\beta$ region) followed by

* Where appropriate, micrographs of NAB are used to illustrate aspects of the binary Cu-Al system.

water quenching.

As noted by Brezina,".....systematic investigations under practical conditions of the mechanical properties and corrosion resistance have shown that it is not very important whether martensite, coarse bainite or fine bainite are present". Hence, the term α_1' will be used to describe "martensite" in both the binary and NAB systems. The small, geometrical pools of martensite in Figure 4 are most likely α_1"; however the generic term α_1' will be used. The designation α^* is introduced below and will be used to describe intimate mixtures of both martensite and bainite.

α_B: *is designated as bainite*. Smith and Lindlief [18] demonstrated the appearance of a supersaturated, plate-like α phase (α_B on Figure 2): (the high-temperature, proeutectoid alpha phase is rod-like): however, the term bainite was not employed. Haynes [25,26] documented the appearance of a "fine acicular form" of α (bainite), in a series of Cu-Al-(Ni) alloys, at temperatures ~100°C below the eutectoid. This bainitic α formed together with the "Widmanstatten form" which was observed at higher transformation temperatures. Figure 6 is a light micrograph of plates of bainitic α, α_B, in a martensitic matrix, the dark etching phase. (The NAB had been solution treated at 1025°C and subsequently water quenched).

In a subsequent study on the nature of proeutectoid and bainitic alpha, Flewitt and Towner [21] examined a series of Cu-Zn alloys and documented the presence of plates of α (bainite), at intermediate transformation temperatures (Figure 7). Given the similarity between both the microstructures and kinetics of the two studies, the designation α_B on Figure 2 appears to be appropriate.

α : a mixed microstructure.* Brezina [1] discussed the formation of bainitic plates of alpha in binary Cu-Al alloys as shown in the schematic diagram of Figure 8, which describes the formation of a "mixed microstructure" in a hypoeutectoid Cu-Al alloy. During the cooling cycle, (e.g., air cooling), the high temperature β can phase-separate above 500°C to produce plates of bainite in the β matrix. Subsequently, the β can start to order (i.e., β_1 forms) and eventually the remaining β_1 will transform to martensite (α'_1). The result is a microstructure consisting of both martensite and bainite. Brezina [1] used the term α* to describe such a complex mixture. As shown in Figure 6, bainite/martensite mixed microstructures can be very common: hence, it is suggested that the designation α* be retained.

2.2 Continuous Cooling Transformation (CCT) Curves and Microstructure Maps.

Brezina [1] presented a wide-ranging kinetic and microstructural study of a series of Cu-Al binary alloys, Cu-Al-(X) ternaries and Cu-Al-(X)-(Y) quaternary alloys. This section presents a brief review of Brezina's methods for the acquisition of kinetic data and his methods of their presentation; namely CCT curves and microstructure maps. The results are for binary Cu-Al alloys.

Critical temperatures (e.g., that for the onset of the $\beta_1 \rightarrow \alpha_1'$ reaction) were determined using a combination of dilatometry and differential thermal analysis (DTA) [22]. Figure 9 is a DTA scan for an eutectoidal Cu-Al binary alloy. The three exothermic peaks correspond to the transformations indicated on the Figure (and see below). Electrical resistivity and magnetic measurements were also cited [22], but it appears that the bulk of Brezina's work employed the former two techniques. Brezina employed "small" samples

(11mm x 1mm coupons) but used simulation techniques [23] to predict cooling conditions for commercial practices (e.g., cooling a 200mm thick plate in oil) from the cooling times achieved in the laboratory. The resultant data of Brezina [23] are presented in Figure 10. Finally, standard metallographic techniques were used to identify various phases and microconstituents.

Figures 11a, b are a microstructure map (a) and the corresponding CCT curves (b) respectively, for an eutectoidal Cu-Al alloy. Brezina [1] was perhaps the first to present CCT curves that are "read" from top to bottom, as opposed to from top left to bottom right. Later, the practice was adopted by British Steel in their landmark publication of ref [24].

The microstructure maps (μmaps) were also novel at the time of Brezina's original publication but are now seeing increased usage in e.g., the steel's literature. The use and utility of Figures 11a, b can be gauged with respect to the cooling time of 2×10^3s which is represented by the vertical line on the above mentioned figures. Figure 11b indicates that the decomposition of the β begins at ~550° C with the formation of the eutectoidal mixture of $\alpha+\gamma_2$. Shortly thereafter, the matrix begins to order to the β_1 phase (these two transformations correspond to the first exothermic peak on Figure 9). At ~475° C, bainitic plates of α_B begin forming in the β. Continued formation of $(\alpha + \gamma_2)$ plus α_B persists until the martensite start temperature (Ms) is reached at ~275° C (Figures 9 and 11b), at which point the reaction $\beta_1 \rightarrow \alpha_1'$ initiates. At ~ 180° C, the decomposition of the β/β_1 is completed. The microstructure consists of a mixture of the eutectoid product $(\alpha + \gamma_2)$, bainite (α_B) and martensite (α_1'), as is shown in Figure 11a; ~30% $(\alpha+\gamma_2)$ co-existing with ~70% α*. Note that Brezina [1] does not differentiate between bainite and martensite

(Section 2.1) and we can describe the microstructure α * as:

$$\alpha^* = \alpha_B + \alpha_1'$$

The data presented in Figures 11a. b are broadly consistent with the TTT curves of Figure 2: Figure 2 predicts that the high temperature transformation product/microconstituent is α + γ_2, the ordering reaction then commences, to be followed by the bainite reaction (the martensite reaction is not alluded to in Figure 2).

To facilitate later discussions on the more complex ('hypoeutectoid"), NABs, Figure 12 presents CCT curves and μmaps for a hypoeutectoid Cu-Al alloy, upon which the cooling time of $2x10^3$s has been inserted. For this arbitrarily chosen cooling time, the resultant microstructure consists of ~ 60% proeutectoid α, ~35% α^* (the plate-like mixture of bainite plus martensite) together with a small amount of the eutectoidal mixture of $\alpha + \gamma_2$

3. The Nickel-Aluminum Bronze (NAB) System: Proposed Terminology.

3.1 The Cu-Al-Ni, Cu-Al-Fe and Al-Ni-Fe Ternary Phase Diagrams.

Figure 13 presents isothermal sections of the three ternaries which are relevant to the Cu-Al-Fe-Ni, NAB system. Figure 13 has been adapted from ref.[5] with a terminology which is consistent with that shown in Tables I and II. The relevant intermetallics are:

γ_2:	the binary intermetallic in the binary Cu-Al system (Figure 1)
γ' :	based on Ni_3Al. Its presence has not been documented previously in the NABs.
κ_{II}:	based on Fe_3Al (and see sections 3.2 et seq.)
κ_{III}:	based on a NiAl. This phase has a very broad composition span, ranging from NiAl to FeAl.

Assuming that no further intermediate phases are present in the quaternary system: the above listing should, at the very worst serve as an excellent guide to the equilibrium precipitate phases that could form in slowly cooled NAB.

3.2 The Kappa Phases in Slowly Cooled NAB

Table II presents the proposed terminology for the precipitate species which can form in *slowly-cooled* Cu-Al-Fe-Ni bronzes* . The phases/microconstituents with which they may be associated are those listed in Table I. i.e., the proposed terminology embraces all of the entities listed in Tables I and II (with the exception of κ_V : see Table II and below). The following is a list of the precipitate species together with pertinent structural information. To facilitate the following discussion, Figures 14 and 15 present "schematic microstructures" of NAB castings for both "high-Fe" containing NAB (Figure 14) and for more conventional NAB (Figure15).

κ_{II} : *are dendritic* (variously called globular or rosette) in morphology and are formed in the β phase (i.e., by a solid state reaction). Figures 16a, b are light micrographs of slowly cooled (cast) NAB. The dendritic (also called rosette) particles are κ_{II} precipitates. κ_{II} particles are not single phase at room temperatures (e.g., see Figure 16b), but are based on the Fe_3Al (DO_3 structure) with a = 5.71± 0.06 Å [4]. It is suggested that κ_{II} does form as a single phase when precipitating in the β. (It is likely that the stoichiometry range of the κ_{II} phase decreases with decreasing temperature). Its presence as an equilibrium phase in e.g., the Al-Ni-Fe system is well documented (Figure 13), and its dendritic morphology

* The data from which Table II was generated was presented, primarily by Lorimer, Ridley and co-workers [2-9]

has been discussed in ref. [27]. κ_{II} particles tend to form within the same temperature range as the Widmanstatten α (Section 3.4) . Hence, the κ_{II} precipitates are frequently associated with either the $\alpha + \kappa_{III}$ eutectoid (Figures 16a, b) or with high-Al martensite (Figure 17). The crystal structure of the κ_{II} phase is shown in Figure 18. Note that it is an "ordered version" of the disordered, high temperature β phase: this in part, explains its dendritic morphology.

Reference to Figure 16b shows, that, indeed the κ_{II} particles are multiphase and there appears to be a relatively sharp transition in etching behaviour between the center and periphery of the dendritic particles. This etching behavior suggests that a κ_{II} to κ_{III} transition occurs during precipitate growth of the solid-state dendrites. Evidence for this transition has been provided by e.g., refs. [10-12]. The wide stoichiometry ranges of both the κ_{II} and κ_{III} phases, together with their similar crystal structures (Figure 18) would favor such a transition.

κ_{III} : *the binary eutectoid reaction product*, forms as:

$$\beta \rightarrow \alpha + \kappa_{III}$$

Hence, the κ_{III} tends to be either lamellar or discrete (Figures 16a, b and see Figures 14 and 15). κ_{III} is based on NiAl (B2 structure) with a lattice parameter of 2.88 $\pm$ 0.03 Å (and see Figure 18 [4]). The κ_{III} phase is structurally identical with the NiAl phase which is found in ternary Cu-Al-Ni alloys (Figure 13 and see [25,26]). It is likely that the κ_{II} particles can act as a substrate for the formation of κ_{III} particles (e.g., see Figure 16b): both are "ordered

versions" of the high temperature β phase (Figure 18).

κ_I: *are "large, dendritic-shape" particles* that only form in NABs with a high iron content [4] of greater than ~5% and/or a high Fe: Ni ratio [12]. It would appear that the κ_I particles form in the melt, are normally located in the centers of α grains and are multi-phase (Figures 19a,b). Jahanafrooz et al [4] documented the presence of Cu-rich precipitates, bcc Fe-rich precipitates, DO_3 (Fe_3Al) and B2 (FeAl) particles in single dendrites of the κ_I microconstituents. Although it may be argued that κ_I should not be considered a "phase"; it most certainly is not a single phase at room temperatures, it is highly probable that it was formed as a single phase from the melt, (as κ_{II}), but then subsequently phase separated. κ_I is not found in "normal chemistry" bronzes. Although most likely based on κ_{II}, it is suggested that the designation κ_I be retained, as it deliniates a microconstituent that most probably forms from the melt and not in the solid state.

Figures 19 a,b are low magnification, light microscope images of an atypical, high-Fe casting which contains dendritic κ_I precipitates (the dark etching constituent). As noted above, the κ_I particles form in the melt. (Studies at Penn State have shown that the κ_I phase is stable above the solidus temperature [12]). Additionally, it is likely that they transform partially to the β phase, during cooling, via the peritectic reaction:

$$L + \kappa_I \rightarrow \beta$$

Reference to Figures 19 a,b, also indicates the presence of the proeutectoid α phase (the light etching microstructural constituent) encapsulating the κ_I, together with pools of the eutectoidal mixture of $\alpha + \kappa_{III}$.

κ_{IV} : *particles*, it is most unlikely that the κ_{IV} constituent is distinct from κ_{II}. κ_{IV} forms in the α, but has a structure and composition which is very similar to that of κ_{II} (Tables II - IV). Although κ_{II} and κ_{IV} appear to be one and the same, it is suggested that the designation κ_{IV} be retained, if for no other reason than its widespread use. κ_{IV} precipitate free zones are invariably encountered at the periphery of the α grains; wherever κ_{II} and/or κ_{III} are present (Figures 16a,b). The κ_{IV} particles are discrete, displaying spherical, cuboidal or even cruciform morphologies (Figure 20). They may also be internally twinned.

κ_V : *the κ_V "phase"* has been reported during the tempering of NAB [1,14,16]. However, κ_V is structurally identical to κ_{III} (see section 3.3). It is suggested that its use be discontinued. Figure 21 is a light micrograph of "lath-like" particles of κ_{III} in a tempered NAB.

3.3 Compositional and Structural Aspects of the κ Phases.

A number of authors have presented information on either the structural nature of the κ phases and/or their composition ranges (e.g., see refs. [2,4-7,14,16]). By far the most comprehensive structural and compositional analyses of the κ phases were performed by Lorimer, Ridley and co-workers [4-7], using transmission electron microscopy, (TEM), and a precis of their data is presented in Tables III and IV*. Perhaps most telling, the

---

* In Table III, and all subsequent tabular material, the designation of e.g., "cuboidal/cruciform" under the heading "Morphology" implies the presence of two distinct morphologies as opposed to two equivalent descriptions of a single shape. For example, the κ_{IV} precipitates undergo a morphological transformation, during coarsening, from cuboidal to cruciform.

selected area diffraction pattern (SADP) data only supports the presence of the two distinct kappa phases: namely κ_{II} and κ_{III} (Table III). These two structures, DO_3 and B2 respectively (Figure18), correspond with those which would be expected to occur from the ternary phase diagrams of Figure 13.

Table III has been divided into two groups; the κ phases which have the DO_3 (Fe_3Al) structure and those which have the B2 (NiAl) structure. In the former category κ_{II} is considered to be the "prototype" and precipitates in the β phase (Table II). The " κ_I phase" most probably forms in the melt, and κ_{IV} forms in the α phase.

The prototypical B2 (NiAl) phase is the eutectoidal κ_{III} constituent which adopts either a lamellar or spherical morphology. Culpan and Rose [16] attempted to differentiate between these two morphologies. However, based on both their structural identities (confirmed in e.g., refs. [6,7]) and their very similar chemistries (Table V), no differentiation is warranted.

What may be termed "martensitic" κ_{III} forms in association with the islands of high-Al martensite in the as-cast, or slowly cooled conditions. Finally, the lath-like κ_{III} (referred to as κ_V by e.g., refs. [14, 16]) precipitates within both the α phase and the martensite during tempering (Figure 21).

The compositional analyses (again performed on the TEM which minimizes erroneous signals) can be grouped as per Table III, and are shown in Table IV. Two distinct kappa phases only, may be distinguished. The data in Table IV are presented as both atomic % and as weight % (the latter in parentheses). The Ni:Al and Fe:Al ratios

clearly show the presence of two distinct phases only, both of which have relatively wide composition ranges (and see the ternary phase diagrams of Figure 13).

3.4 Vertical Sections of the Cu-Al-5%Ni-5%Fe Phase Diagram.

Figure 22 is a vertical section through the Cu-Al-Ni-Fe phase digram, as determined by Cook et al. [13]. The phase diagram was constructed from a very careful study of a series of different Cu-Al-Ni-Fe alloys which had been solution treated at 1000° C, cooled to various lower temperatures and subsequently quenched. This vertical section (one of four) was interpolated from the microstructure maps shown in Figure 23. Hence, it can be concluded that the phase diagram in Figure 22 is, at least, qualitatively correct. However, Cook et al., [13] did not differentiate between κ_{II} and κ_{III} : the generic term κ, being used.

The only other vertical section of the quarternary phase diagram appears to be that due to Brezina [1]. Unfortunately his diagram (Figure 24) appears to have been heavily influenced by Cook et al., [13], and the corresponding solvus lines match almost exactly. Even more unfortunate is the fact that Brezina opted to employ the generic description of κ even though his terminology, in the body of the text, admits to the presence of e.g., κ_{II} and κ_{III}.

In an effort to produce a more realistic vertical section of the NAB phase diagram, the data of ref. [13] have been reinterpreted in terms of the precipitation of two κ phases: κ_{II} and κ_{III}. The results are presented in Figure 25: the solvus lines of ref. [13] have been retained, however, the phase fields have been re-labelled in accordance with the proposed terminology of e.g., Tables I and II. The assignment of κ_{II} to the high temperature, high aluminum phase field was based on examination of the micrographs contained in the

various publications of Lorimer, Ridley and co-workers [3-9], and by students at Penn State ([10-12]).

3.5 Quenched/Quenched and Tempered NAB.

Depending on the quenching rate, bainitic and/or martensitic microconstituents are predicted to form in most quenched NABs (e.g., see Figures 11,12,27,28). Swan and Warlimont [20] identified three different martensite structures in binary Cu-Al alloys (Figure 5), and Brezina [1] described the decomposition of binary hypoeutectoid Cu-Al alloys to a mixture of both bainite and martensite (termed α^*) during air cooling: a good example of this latter microconstituent/mixture was presented in Figure 6.

Swan and Warlimont determined that the martensite start temperature (M_s) decreased with increasing aluminum content (Figure 5). However, Cook et al. [13] showed that the "hardenability" * of NAB increased with increasing %Al. For example, it was found that a substantial fraction of "secondary α" (bainite) was found in quenched NAB when the alloy contained 8% or 9% Al: the amount of bainite decreased at 10%Al and was absent in the 11% and 12%Al alloys. Hence, the critical cooling rate for the suppression of the bainite reaction decreases as the aluminum content increases (Alternatively, the hardenability increases).

In NAB material with standard chemistries, it is virtually impossible to create a microstructure that is 100% α_1' (martensite) because of the rapid intervention of the bainite reaction. Indeed, as noted by Brezina "..... it is not possible to obtain a fully martensitic structure in the alloys Cu-10.5Al-5Fe and Cu-10.5Al-5Fe-5Ni even at ..... (rapid) quenching rates (in platelets 3mm thick, immersed in brine)". However, if a fraction of the

---

* Hardenability is a measure of the ease with which a given alloy forms martensite. This terminology has been "borrowed" from the steel's literature

β can be enriched in Al by e.g., the prior precipitation of the proeutectoid α phase. then the alloy hardenability increases. Figure 17 presented a scanning electron microscope (SEM) image of a sample which had been slowly cooled from 1025°C to 823°C and subsequently quenched. The development of the Widmanstatten rods of α, prior to the quench. increased the hardenability of the remaining β to an extent sufficient to form martensite and no bainite: the large dendritic particle in the martensite is κ_{II} . A similar example was shown in Figure 4. In this instance, the alloy was isothermally transformed at 775°C for 15 mins. and subsequently quenched. The isothermal transformation yielded the Widmanstatten rods of proeutectoid α and initiated the eutectoidal reaction. These decomposition products led to the enrichment of the remaining β in aluminum which, when quenched, yielded 100% martensite in the remnant pools of β (i.e., the critical cooling rate for bainite suppression was exceeded). The extent of alloy partitioning during the formation of e.g., proeutectoid α is demonstrated in Table VII

3.5.1 The Effect of Tempering (Subcritical Annealing).

Tempering "martensitic" microstructures has been performed by many previous investigators (e.g., see refs. [5,7,13]). A series of complex reactions can occur, depending on time, temperature and alloy chemistry. However, the overall sequences can be written as:

$$\alpha_I' \rightarrow \alpha + \kappa_{III} \qquad \text{(i)}$$

or:

$$\alpha_I' + \kappa_{III} \rightarrow \alpha + \kappa_{III} \qquad \text{(ii)}$$

depending on the presence (or absence) of κ_{III} in the as-quenched material. In either instance, the resultant microstructure consists of α + discrete κ_{III} particles (Figure 21).

Recognizing the fact that tempering treatments are performed on materials that most likely contain a mixture of proeutectoid α, bainite and martensite, the following reactions will also occur:

$$\alpha_B \rightarrow \alpha + \kappa_{III} \qquad \text{(iii)}$$

$$\alpha + \kappa_{IV} \rightarrow \alpha + \kappa_{IV} + \kappa_{III} \qquad \text{(iv)}$$

Note that in all cases, κ_{III} is precipitated during tempering, i.e., κ_{III} is the "tempering phase". Table VIII lists the phases/microconstituents which are present in quenched/ quenched and tempered NAB. However, it should be noted that after tempering, the only phases remaining are α, κ_{II} and κ_{III}.

3.6 Summary of Proposed Terminology.

Table IX summarizes the proposed terminology and also lists several previously employed nomenclatures. The proposed terminology (Column I) contains those phases /microconstituents which are either deemed to be distinct phases, and/or those whose use is so common that their deletion would appear to be counterproductive. Further information on the designations in Column I can be found in e.g., Tables I and II. Some of the other columns in Table VIII show "large fallow areas". For example, Swan and Warlimont [20] and Smith and Lindlief [18] only examined binary Al-Cu alloys. Conversely, Ridley, Lorimer and co-workers [6,7] only examined the complex NABs: hence the fallow areas. I have tried to be as accurate as possible regarding the terminology of e.g., Cook et al. [13], however, I have had to make various judgements on their original publications.

In summary, it is felt that Table VIII represents a consistent set of terms that should be sufficient for the description of the phases and microstructures in NAB although there is some redundancy, e.g., with respect to the κ_I, κ_{II} and κ_{IV} phases.

4. The Nickel-Aluminum Bronze (NAB) System. Continuous Cooling Transformations and Microstructural Development.

4.1 Continuous Cooling Transformation (CCT) Curves.

A number of authors have described the continuous cooling characteristics of NAB (e.g., [1], [6], [12]). Figure 26 is a schematic diagram of the "order" in which the beta phase decomposes [16] in one particular bronze. The figure has been adapted from Culpan and Rose [16], in accordance with the proposed terminology of e.g., Table IX. However, the transformation sequences are dependant, both on the chemistry of the bronze and on the cooling rate. Brezina [1] presented both CCT curves and μmaps for a series of nickel-aluminum bronzes and two such examples are presented in Figures 27 and 28. Reference to Figures 27a,b shows that moderately slow cooling ($2x10^3$s cooling time) of the 9%Al-5%Fe-5%Ni alloy will yield a microstructure consisting of ~ 55% proeutectoid α rods, 35% of the eutectoid mixture of $\alpha + \kappa_{III}$ and ~ 10% α* (Figure27a). Note also that during cooling, precipitation of Widmanstatten α in β precedes the formation of dendritic κ_{II} in β (Figure 27b).

In the alloy with a higher Al content (Figure 28), the κ_{II} phase is the first phase to appear in the β, during cooling from 1000°C (Figure 28b). The fraction of proeutectoid α in the microstructure decreases in comparison with that obtained in the lower Al alloy

(Figure 27a), and there is a corresponding increase in both the fraction of the eutectoid (see below), and the α^* microconstituent (the intimate mixture of bainite plus martensite).

Although not specifically alluded to in ref. [1], it is possible to use the CCT curves and μmaps of e.g., Figures 27 and 28 to design, albeit tentatively, heat treatments that will produce specific microstructures in NAB. The following describes a rationale for predicting solution treatment temperatures and aluminum contents which would produce varying volume fractions of the eutectoid microconstituent. Section 4.2 then describes a series of "real microstructures" that may be developed in NAB.

The CCT curves of ref.[1] (see e.g., Figures 27b and 28b) may be used to estimate the critical temperatures for the formation of α and κ_{II} on cooling (the Ar temperatures) and by extension, the minimum temperatures for full solution treatment (reforming 100% β) on heating. These data are plotted in Figure 29a. In all cases, the Ar temperatures were estimated from the slowest cooling rates employed in ref. [1]. A comparison of Figure 29a with the phase diagrams of Figures 24 and 25 shows good qualitative agreement, with the $\beta/\beta + \alpha$ solvus increasing with decreasing aluminum content. Reference to Figure 29 also indicates that an annealing temperature of $\equiv$ 1000° C would be needed to yield 100% β (i.e., a full solution or "*supercritical*" treatment) for alloys containing ~ 8 - 9%Al.

In designing microstructures, a knowledge of the volume fraction of the eutectoidal mixture of $\alpha + \kappa_{III}$ is of import. Figure 30 plots the percentage of the eutectoid microconstituent as a function of aluminum content. The data have been estimated from the μmaps presented in ref.[1] (and see Figures 27a and 28a). The data were obtained for a slow, somewhat arbitarily chosen cooling rate which corresponds to the sand casting of a 200mm thick plate. This cooling rate minimized the amount of bainite/martensite (α^*) that

would form in the alloy; however, some $\alpha + \gamma$ eutectoid product is included in the data of Figure 30. The major trend is a decrease in the volume fraction of eutectoid product with decreasing aluminum content; it is predicted that the microstructure should contain virtually no $\alpha + \kappa_{III}$ below approximately 8%Al. Figure 31 is a light micrograph of a NAB casting which contained ~ 7.8% Al: no eutectoid is present. However, the grain boundaries are associated with an almost continuous film of κ_{III}. Note also the κ_{IV} in the body of the α grains.

4.2 Microstructures and Microstructural Develoment in NAB.

The following sub-sections briefly describe microstructural development in NAB with respect to a series of continuous cooling protocols. The protocols are developed in association with a "hypothetical μmap". It is then shown that the attainment of certain microstructures may be facilitated by *intercritical*, as opposed to *supercritical* annealing prior to continuous cooling.

Figure 32 is a hypothetical microstruture (μmap) of an alloy which contains ~9.5% Al-5%Fe-5%Ni. Superimposed on this μmap are six different cooling curves (1-6), each of which, at least potentially, can result in an "unique" microstructure. Although Figure 32 is schematic, it is at the very least, qualitatively correct and predicts the observed sequences of transformation products as a function of cooling rate. Figure 32 also differentiates between martensite (α_1') and bainite (α_B), with bainite predominating at the intermediate cooling rates.

4.2.1. Microstructure I: Proeutectoid α+ The Eutectoid Mixture.

Very slow cooling (e.g., for a large casting) will yield a microstructure which

consists of proeutectoid α, together with the eutectoid mixture of $\alpha + \kappa_{III}$ * (Figures 16a,b).

4.2.2. Microstructure II: Proeutectoid α + The Eutectoidal Mixture + Martensite.

Moderately slow cooling of e.g., a small casting will yield a microstructure which is characteristic of many " slowly cooled", cast NAB; small fractions of the casting transform below M_S to form "high-Al martensite" (and see the schematic drawings of Figures 14 and 15). Partitioning of e.g., Al during the formation of proeutectoid α ensures the formation of a high-Al martensite, with little or no bainite formation.

Microstructures I and II can be developed by simple control of the casting conditions and may not need any further heat treatments.

4.2.3. Microstructure III: Proeutectoid α + Martensite.

Increasing the cooling rate over that necessary to produce Microstructures I and II may produce Proeutectoid α + Martensite . At first sight, this might appear to be "out of sequence" in that the bainite reaction would typically precede the martensite reaction. However, the formation of proeutectoid α increases the hardenability of the remaining β, thereby favoring the martensite reaction. Microstructure III can be obtained by conventional continuous cooling and is frequently developed during welding: (Figure 33). A simpler method of producing alpha plus martensite microstructures is by *intercritical annealing* slowly cooled samples. Reference to Figure 29b shows that if a 9.5%Al NAB is *intercritically* annealed between ~ 850°C and 930 °C, the eutectoid $\alpha + \kappa_{III}$ will revert to β. On subsequent quenching (rapid cooling) the high-Al β will transform predominantly to martensite (α_I'). Figure 34 is a light micrograph of NAB which had been *intercritically*

* This "microstructure" will also contain ~ 3% κ_I [12]. No martensite would be expected.

annealed at 870°C followed by an oil quench. The microstructure consists of proeutectoid α plus martensite (some bainite plates are also observed in the martensite pools).

4.2.4. Microstructure IV: Proeutectoid α + Martensite + Bainite.

Microstructure IV can be attained through continuous cooling (Figure 32). However, *intercritical annealing* will again yield superior results. Figure 35 shows the same NAB as that shown in Figure 34. This latter sample was also annealed at 870° C. but was subsequently air-cooled. The more moderate cooling rate allowed for the development of a higher fraction of bainite. Similar microstructures may be obtained by reducing the overall aluminum content of the alloy.

4.2.5. Microstructure V: Martensite + Bainite.

In the laboratory, this microstructural entity may be obtained by a simple *supercritical anneal* plus quench cycle. An example of this microstructure has been shown in Figure 6. However, it may only prove to be possible to obtain this microstructure in relatively thin samples.

4.2.6. Microstructure VI: Martensite.

To the author's knowledge, it is impossible to produce 100% martensite, using standard quenching techniques, in NAB which contains less than ~ 10% Al.

5. Concluding Discussion.

The phases that form in complex nickel-aluminum bronzes (NAB) can be predicted with reasonable certainty from a knowledge of the phases which form in Cu-rich, binary Cu-Al alloys (Section 2) and in the Cu-Al-Ni, Cu-Al-Fe and Al-Ni-Fe ternary systems (Section 3.1). All room temperature phases/microconstituents are derived from the high temperature, secondary solid solution; the bcc β phase.

During "slow" cooling, the β phase decomposes to form a mixture of the Cu-rich α phase (fcc) and two intermetallic "κ phases" which are based on either the NiAl prototype (κ_{III}) or the Fe_3Al prototype (κ_I, κ_{II} and κ_{IV}). It is also possible to form small regions of high-Al martensite when untransformed β is cooled below the martensite start (M_S) temperature.

During "intermediate cooling rates", bainite is formed. This is the least understood, and indeed analysed of all the phases/microconstituents that form in NAB. Quenching yields a mixture of bainite and martensite. However, conventional quenching techniques are not sufficiently rapid to form 100% martensite.

Finally, a whole range of microstructures can be produced by *supercritical anneals* and/or *intercritical anneals*, followed by cooling in different quenching media. Modification to these structures may also involve subsequent *subcritical annealing* (tempering).

Acknowledgments

The author is grateful to The Copper Development Association for commissioning this review and for their patience. The Applied Research Laboratory at the Pennsylvania State University is also thanked for the provision of financial support to three students, whose theses provided the author with the impetus to understand the intricacies of the microstructures of nickel-aluminum bronzes. Kenny Meinert provided expert scientific and technical assistance, and also provided Figures 34 and 35. Wendy Howell deserves a special thank-you for her careful typing of the manuscript. Finally, the author thanks his former students; David Bell, Kathy Petrolonis and Terri Marsico for providing micrographs for this review.

References.

[1] P. Brezina. Int. Met. Rev., (1982), 27, 77.

[2] D.M. Lloyd, G.W. Lorimer and N. Ridley. Met. Tech., (1980), 7, 114.

[3] F. Hasan, G.W. Lorimer and N. Ridley. Proc. Int. Conf. on "Solid-Solid Phase Transformations". The Institute of Materials, London UK., (1981), 131.

[4] F. Hasan, A. Jahanafrooz, G.W. Lorimer and N. Ridley, Met. Trans. A., (1982) 13A, 1337.

[5] F. Hasan, G.W. Lorimer and N. Ridley. J de Physique, (1982), 43, C4-653.

[6] A. Jahanafrooz, F. Hasan, G.W. Lorimer and N. Ridley. Met Trans A., (1983), 14A, 1951.

[7] F. Hasan, G.W. Lorimer and N. Ridley. Met Sci., (1983), 17, 289.

[8] F. Hasan, J. Iqbal and N. Ridley. Mat. Sci. Tech., (1985), 1, 313.

[9] G.W. Lorimer, F. Hasan, J. Iqbal and N. Ridley. Br. Corrosion J., (1986), *21*, 244.

[10] D.E. Bell. MS Thesis, The Pennsylvania State University (1994).

[11] K.E. Petrolonis. MS Thesis, The Pennsylvania State University (1993).

[12] T.A. Marsico PhD Thesis, The Pennsylvania State University (1996).

[13] M. Cook, W.P. Fentiman and E. Davis. J.Inst. Met., (1951-1952), 80, 1364.

[14] P. Weill-Couly and D. Arnaud. Foundarie, (1973), 28, 123.

[15] R. Thomson and J.O. Edwards. AFS. Trans., (1978), 86, 395.

[16] E.A. Culpan and G. Rose. J. Mat. Sci., (1978), 13, 1647.

[17] E.A. Culpan and G. Rose. Br. Corrosion J., (1979), 14, 158.

[18] C.S. Smith and W.E. Lindlief. Trans. Am. Inst. Min. Met. Eng., (1933), 104, 69.

[19] T.V. Philip and D.J. Mack. Trans. Met. Soc. AIME, (1962), 224, 34.

[20] P.R. Swan and H. Warlimont. Acta. Met., (1963), 11, 511.

[21] P.E.J. Flewitt and J.M. Towner. J. Inst. Met., (1967), 95, 273.

[22] P. Brezina. Appendix 2 to reference [1] p 116.

[23] P. Brezina. Appendix 3 to reference [1] p 119.

[24] An Atlas of CCT Curves. British Steel Co. (1973).

[25] R. Haynes. J. Inst. Met., (1953-1954), 82.

[26] R. Haynes. J. Inst. Met., (1954-1955), 83, 105.

[27] D.E. Bell, K.E. Petrolonis and P.R. Howell. "International Trends in Welding Research". Eds. S.A. David and J.M. Vitek. ASM International, (1993). p 301.

Table I

Phases and Microconstituents in Binary Cu-Al Alloys.

(Proposed Terminology)

(Data primarily from refs. [18], [19], [20])

Phase/Microconstituent	Comments
α	fcc, Cu-rich terminal solid solution (an equilibrium phase: Figure 1);
β	bcc, intermediate solid solution (equilibrium phase Figure 1);
γ_2	complex cubic, γ brass structure. Intermediate phase;
β_1	ordered bcc: Fe_3Al structure. Transition phase;
α_1'	martensite, formed by quenching;
α_B	bainite formed at intermediate transformation temperatures;
α^*	an intimate mixture of bainite and martensite;

Table II

Precipitate "Species" in Nickel-Aluminum Bronzes.

(Proposed Terminology)

(Data primarily from refs. [2-9])

Phase	Distinct Entity ?	Retain ?	Comments
κ_{II}	YES	YES	**Forms in Al-Fe binary alloys: based on Fe_3Al. Precipitates in the β Phase.**
κ_{III}	YES	YES	**Forms in binary Al-Ni alloys: based on NiAl. Precipitates in association with α during the eutectoid decomposition of the β. Also forms during quenching and tempering.**
κ_{I}	NO	YES	Only Forms in Alloys containing in excess of 5%Fe. Probably forms from the melt. Multiphase at room temperature. Most likely based on $\kappa_{II}(Fe_3Al)$.
κ_{IV}	NO	YES	Based on the κ_{II} (Fe_3Al) phase. Forms in the α
κ_{V}	NO	NO	*Occurs during tempering. Based on κ_{III}. Its use should be discontinued.*

Table III

Structural Data on the κ - Phases in NAB.

(Data from refs. [4-7], [10-12])

	Morphology	Structure
κ_{II}	Dendritic	
κ_{IV}	Cuboidal/Cruciform	Fe_3Al DO_3 : a = 5.71Å
κ_{I}	Dendritic	
κ_{III}	Lamellar/Spherical	
κ_{III} *	Spherical	NiAl B2 : a = 2.88Å
κ_{III} **	Lath	

* Spherical κ_{III} that forms in martensite in the as-cast condition.

** Lath - like κ_{III} formed in the α during tempering

Table IV

Typical Chemical Compositions in Atomic% (Weight % in Parentheses) of the κ-Phases in NAB.

(Data abstracted from refs. [6] and [7])

	Ni	Fe	Al	Cu	Ni:Al	Fe:Al
κ_{II}	7 (8)	53 (61)	22 (12)	9 (12)	0.32	2.4
κ_{IV}	6 (7)	64 (73)	19 (11)	2 (3)	0.32	3.4
κ_{I}	3 (4)	66 (72)	18 (9)	8 (11)	0.17	3.7
κ_{III}	32 (41)	10 (13)	44 (27)	12 (17)	0.73	0.23
κ_{III}*	26 (35)	11 (14)	46 (28)	14 (20)	0.57	0.24
κ_{III}**	32 (42)	12 (15)	47 (29)	9 (13)	0.68	0.26

* Spherical κ_{III} in martensite in the as-cast condition.

** Lath-shaped κ_{III} formed in the α during tempering

Table V

Compositional Data (weight %) for Lamellar and Spherical, Eutectoidal κ_{III}

(Data Abstracted from ref. [16])

		Ni	Fe	Al	Ni:Al	Fe:Al
κ_{III}	(Lamellar)	28	22	22	1.27	0.79
κ_{IV}	(Spherical)	24	34	18	1.33	1.89

Table VI

Morphological Characterization of the κ-Phase in NAB

(Data from refs. [4,7,14-16])

	Proposed Nomenclature	Previous Nomenclature
κ_{II}	dendritic	globular [14], rosette [16], nodular [15], dendritic [4, 5,15]
κ_{IV}	cuboidal/cruciform	spherical/small rosettes [16] equiaxed [4, 5]
κ_{I}	dendritic	dendritic [4, 5]
κ_{III}	lamellar/spherical	lamellar/globular [4, 5,16] lamellar/granular [15]
κ_{III}*	spherical	spherical [7]
κ_{III}**	lath	lath

* Spherical κ_{III} that forms in martensite in the as-cast condition.

** Lath-like κ_{III} formed in α during tempering

Table VII

Partioning data for NAB

(Data from ref[11])

	Composition (wt %)				
	Al	Fe	Ni	Mn	Cu
Alloy	9.2	3.8	4.5	1.4	Bal.
Proeutectoid Alpha	7.3	3.6	3.7	1.0	Bal.
Martensite	10.6	4.0	5.8	1.2	Bal.

Table VIII

Microconstituents in Quenched / Quenched and Tempered Nickel-Aluminum Bronzes.

(Proposed Terminology)

(Data primarilly from Refs. [5] , [7], [20])

Phases/Microconstituents	Structure	Comments
Martensite		
α'	fcc	(low Al): faulted
α_I'		
α_I'	ordered tetragonal	(medium Al): faulted
α_I''	ordered orthorhombic	(high Al): twinned
Bainite		
α_B	fcc ?	?
Tempering Phase		
κ_{III}	NiAl	Forms during tempering. Also, present in as-quenched high Al martensite.

Table IX

Proposed and Previous Terminologies for the Phases and Microconstituents in NAB.

Proposed	Name	Swan Warlimont [20]	Smith/ Lindlief [18]	Brezina [1]	Weill-Couly [14] Culpan Rose [16]	Thompson Edwards [15]	Cook et al. [13]	Ridley Lorimer [6,7]
α		α	α	α	α	α	α	α
β		β	β	β	β	β	β	β
γ_2		γ_2	δ	γ_2		γ_2	δ	
β_1	Ordered	β_1	β'	β_1				
α_1'	Martensite	β' β'_1 γ'		β'_1	β' Retained β'/β			Martensite (Retained β)
α_B	Bainite		plate-like α	α'			Secondary α	
α^*	Bainite/ Martensite			β^*	β'			
κ_I				κ_I				κ_I
κ_{II}				κ_{II}	κ_I	Fe-κ	κ	κ_{II}
κ_{III}				κ_{III}	κ_{II} globular κ_{III} lamellar	Ni-κ	κ	κ_{III}
κ_{IV}				κ_{IV}	κ_{IV}		κ	κ_{IV}
				κ_V	κ_V			

THE COPPER-RICH END OF THE COPPER ALUMINUM PHASE DIAGRAM

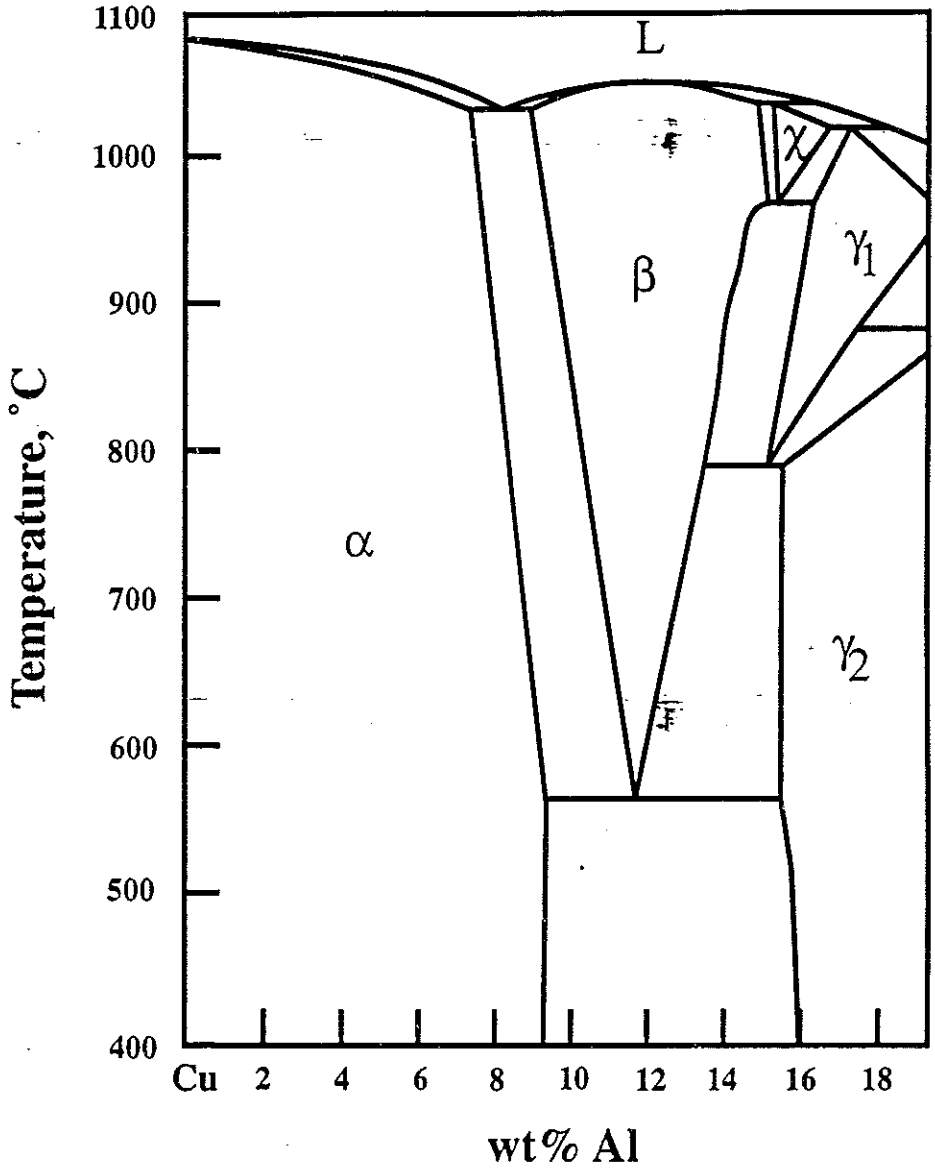

Figure 1. Copper- rich end of the Cu-Al phase diagram The phase diagram is essentially that of Smith and Lindlief [18], but with δ being replaced by γ_2.The α and β phases are identical to those observed in the nickel-aluminum bronzes (NABs).

TTT CURVE FOR AN Cu-11.87%Al ALLOY (SOLUTION TREATED AT 900°C FOR 1 HR.)

Adapted from Smith and Lindlief [18]

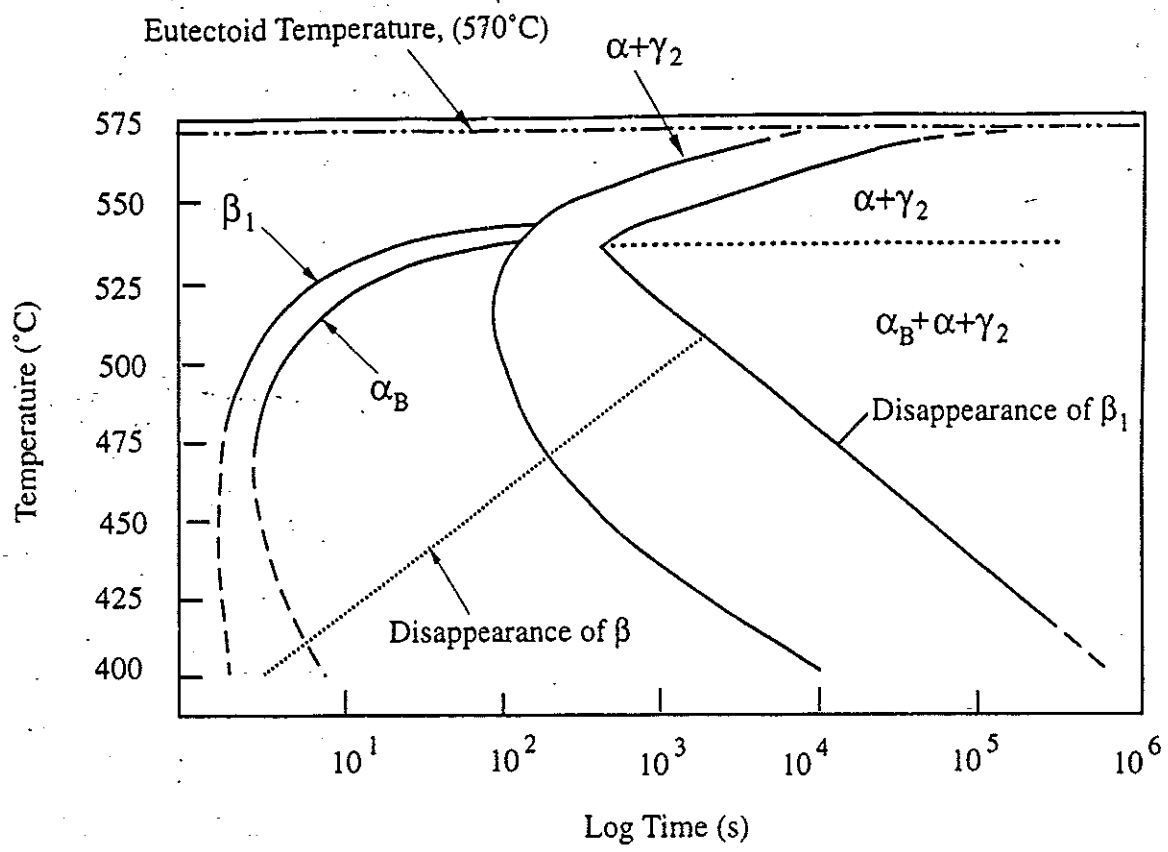

Figure 2. Time-Temperature- Transformation (TTT) curves for a eutectoidal Cu-Al alloy. β_1 is an ordered version of the high temperature β phase, and α_B is bainite.(Adapted from Smith and Lindlief [18]). The terminology in this, and all subsequent Figures is that which is presented in e.g., Tables I and II. Note that Smith and Lindlief did not investigate the martensite reaction.

PROEUTECTOID ALPHA AND THE EUTECTOID MIXTURE

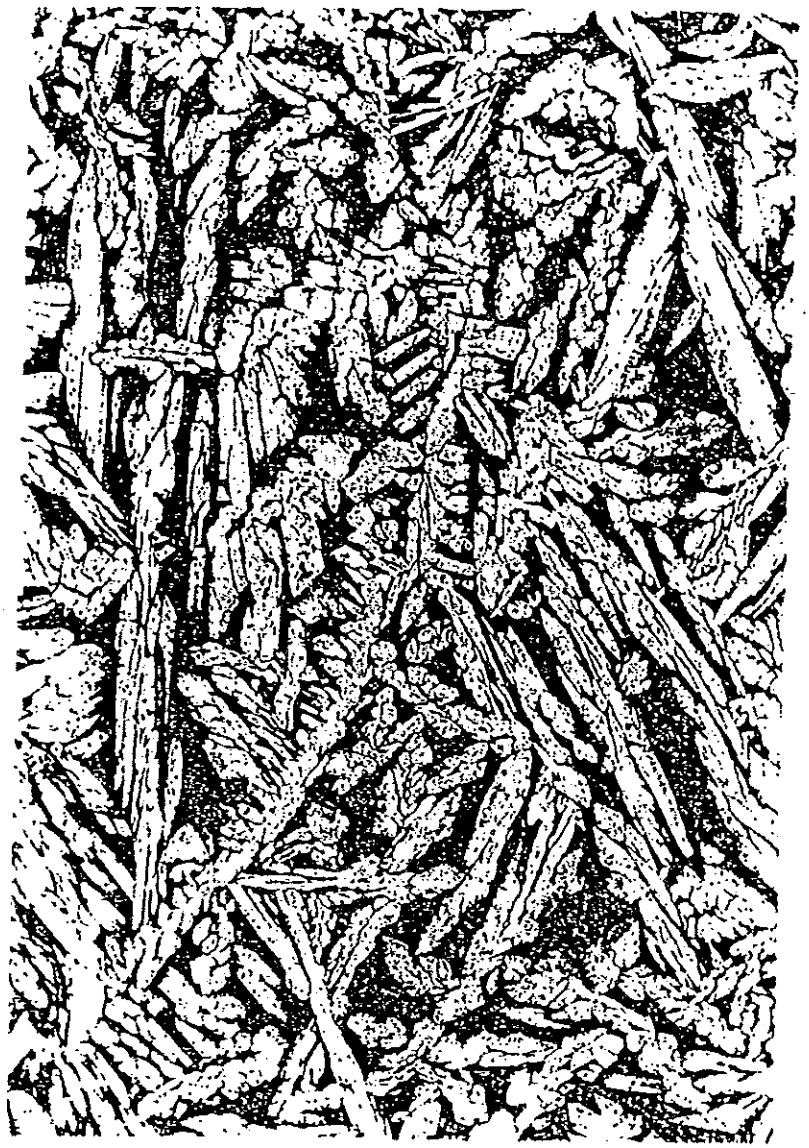

Figure 3. Low magnification light micrograph of slowly cooled NAB. The microstructure consists of rods of proeutectoid α, together with the eutectoid mixture of $\alpha + \kappa_{III}$.

PROEUTECTOID ALPHA, THE EUTECTOID MIXTURE AND HIGH-ALUMINUM MARTENSITE

Figure 4. Light micrograph of slowly cooled, but incompletely transformed NAB, which contains proeutectoid α, small dendritic particles of κ_{II}, the eutectoid mixture of $\alpha + \kappa_{III}$, and encapsulated islands of high-aluminum martensite. The martensite is featureless.

THE COPPER-RICH END OF THE COPPER ALUMINUM PHASE DIAGRAM, SHOWING THE MARTENSITE START TEMPERATUR

(Adapted from Swan and Warlimont [20]

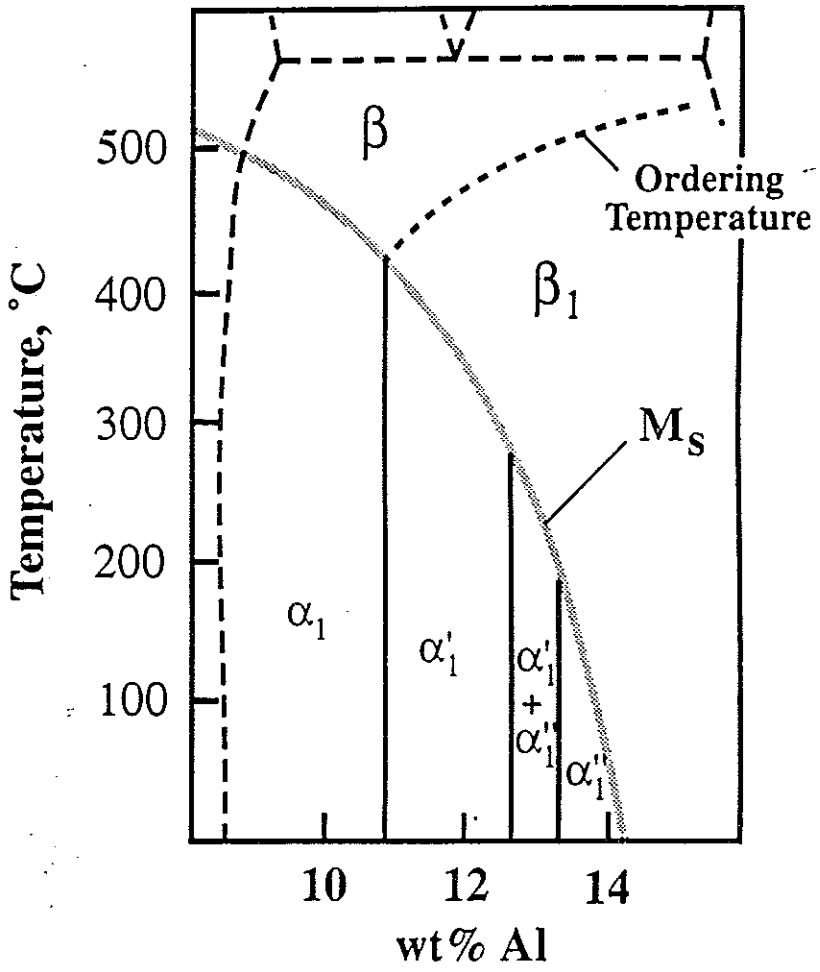

Figure 5. Copper-rich end of the copper-aluminum phase diagram, showing the Martensite start temperature, and the β ordering temperature. The three martensitic structures are referred to collectively, in the text and in subsequent figures and tables, as α'_1. (Adapted from Swan and Warlimont [20])

BAINITE AND MARTENSITE

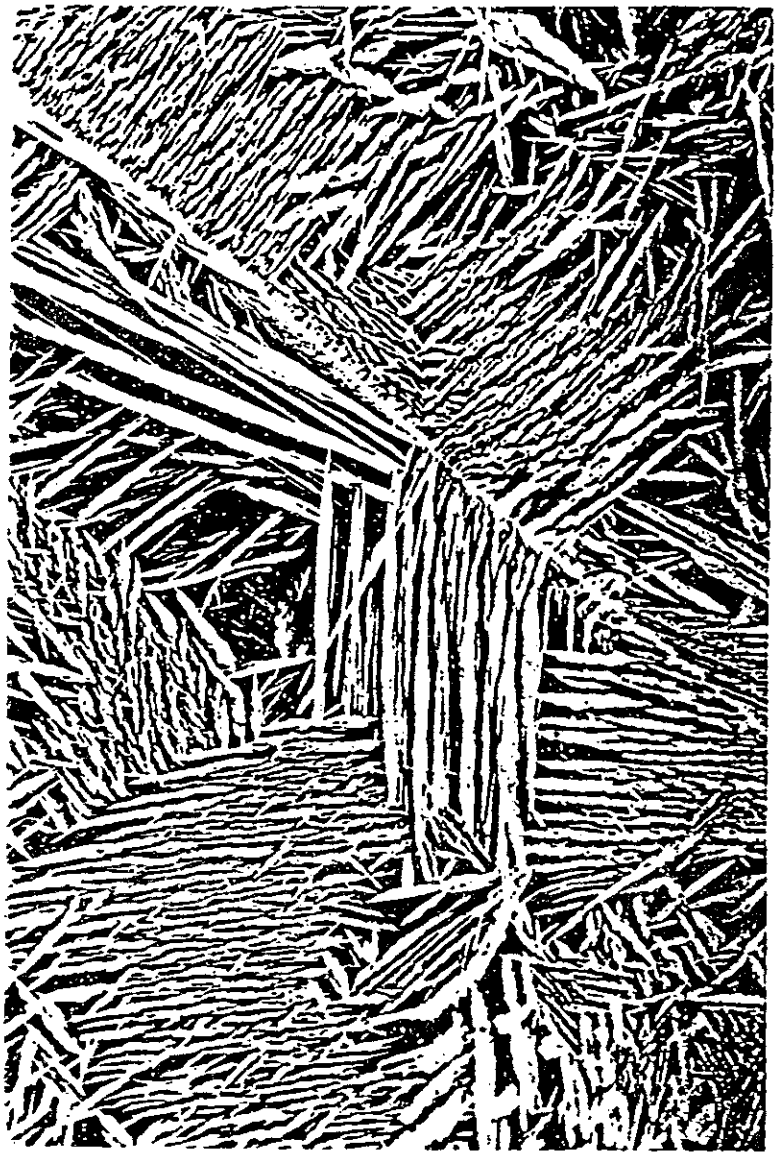

Figure 6. Light micrograph of quenched NAB, which contains plates of bainite (light etching) and martensite.

TTT CURVES FOR A 60-40 ALPHA-BETA BRASS

(Adapted from Flewitt and Towner[21])

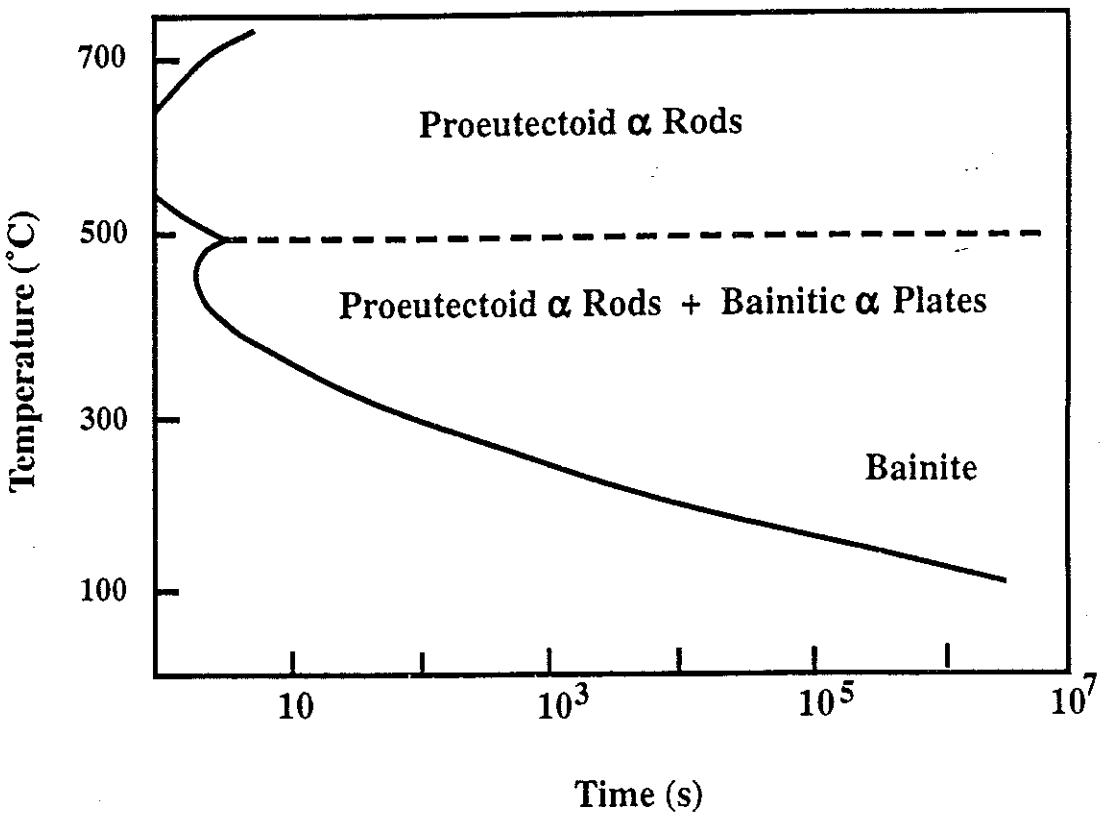

Figure 7. Time-Temperature- Transformation (TTT) curves for a 60-40 Brass. The separate "C"-Curves are indicative of a proeutectoid reaction at high temperatures, and a bainitic reaction at lower temperatures. (Adapted from Flewitt and Towner [21]). The overall similarity in structure, morphology and kinetics between the intermediate temperature transformation products in the brasses, the binary Cu-Al alloy and the NABs, strongly suggests that bainite is formed in all three alloy systems.

THE BAINITIC MICROCONSTITUENT IN HYPOEUTECTOID Cu-Al BINARY ALLOYS AND THE FORMATION OF α*

Adapted from Brezina [1]

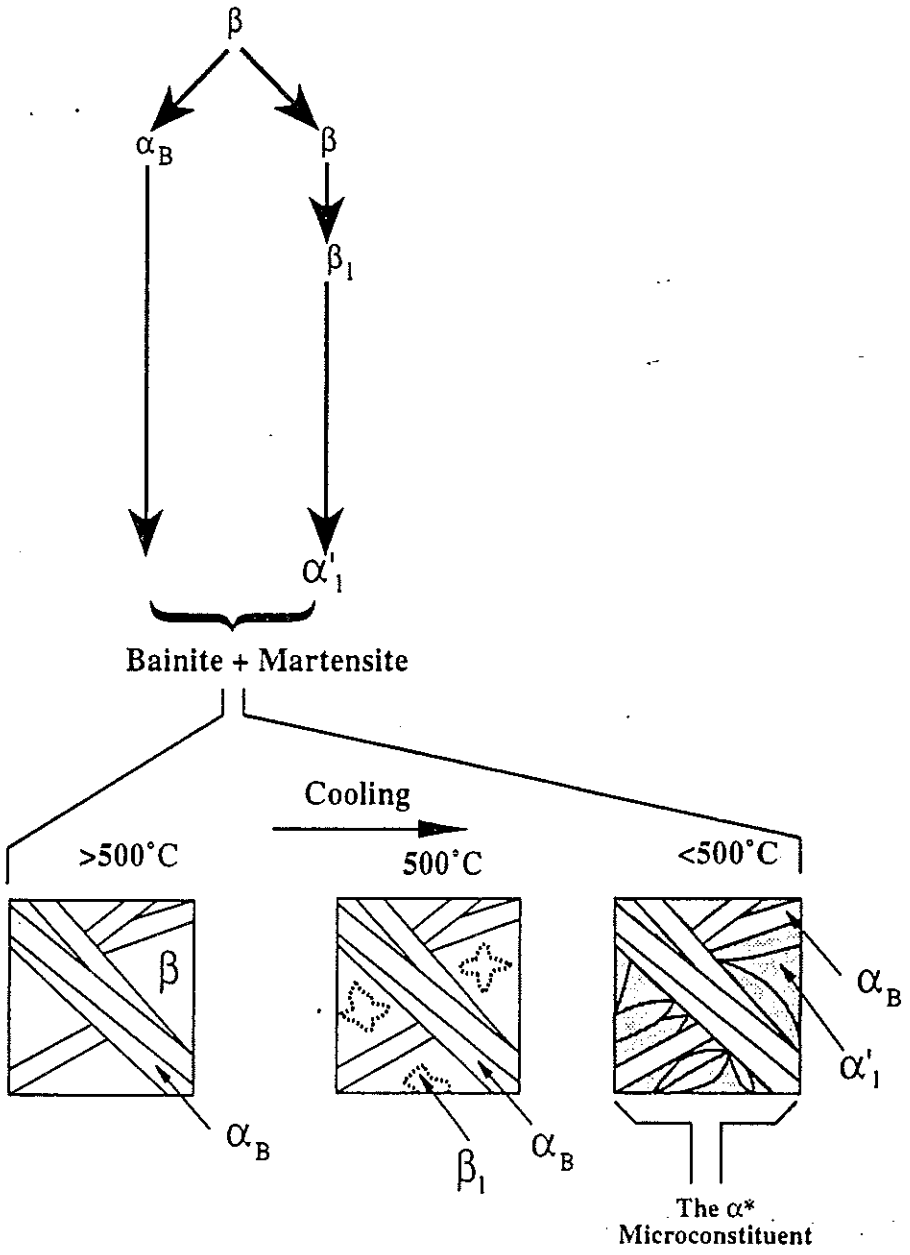

Figure 8. The formation of Bainite during either a moderate cooling rate, or for an intermediate transformation temperature. The bainitic α forms as plates and with a full or partial supersaturation of Al. Although not analysed, it is likely that the bainite is fcc. Typically, the bainite reaction does not go to completion during cooling, and the resultant microstructure is a mixture of bainite and martensite (α*). In addition, it is very difficult to quench severely enough to produce 100% martensite in the NABs, and "rapidly cooled" microstructures invariably contain both bainite and martensite (α*). (Amended from Brezina [1])

DIFFERENTIAL SCANNING CALORIMETRY CURVES FOR A BINARY Cu-Al ALLOY

Adapted from Brezina [22]

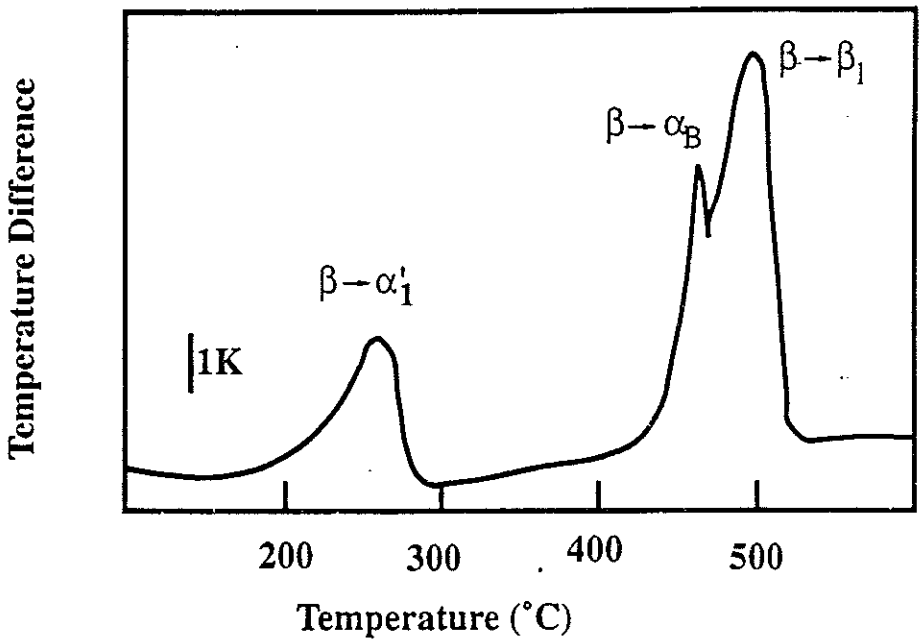

Figure 9. Differential Scanning Calorimetry (DSC) curves for a binary Cu-Al alloy. The three exothermic peaks can be identified with the "critical temperatures" for the $\beta \rightarrow \alpha + \gamma_2$ and $\beta \rightarrow \beta_1$ transformations (overlapping), the bainite transformation ($\beta \rightarrow \alpha_B$) and the martensite transformation ($\beta \rightarrow \alpha'_1$) (Adapted from Brezina [22])

EQUIVALENT PLATE THICKNESSES
(Brezina[23])

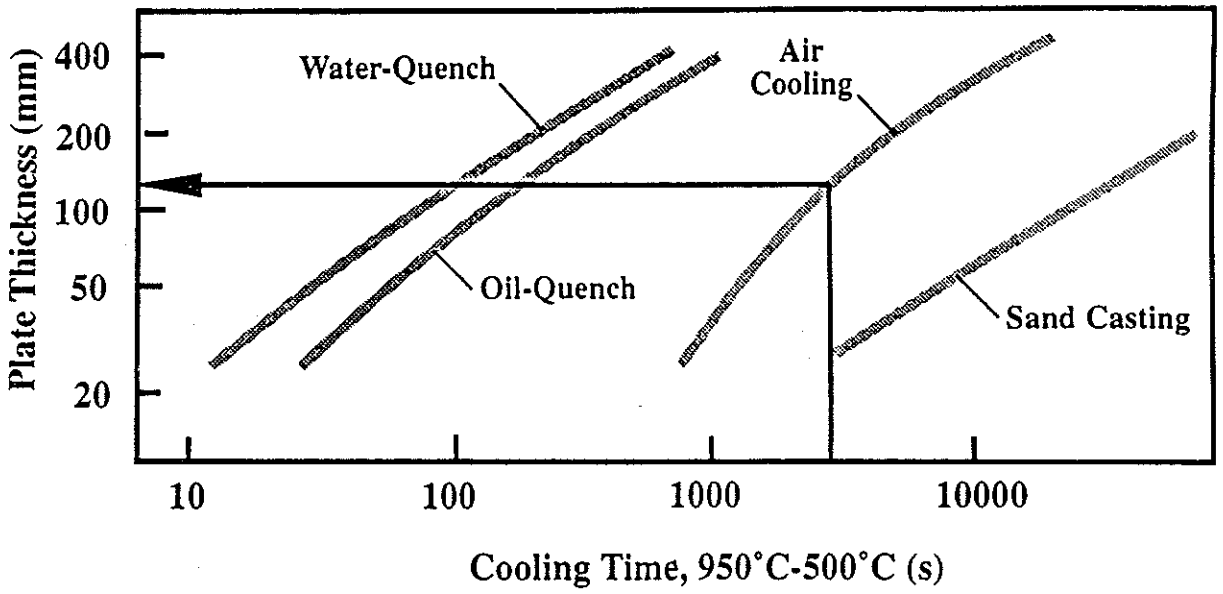

Figure 10. Master curves for the conversion of cooling times to "equivalent plate-thicknesses" and for a variety of cooling media. As indicated on the figure, a cooling time of approximately 2000s (and see figure 11) corresponds to the cooling rate obtained for a 125mm thick plate, cooled in air (Adapted from Brezina [23])

MICROSTRUCTURE MAP AND CCT CURVES FOR A Cu-11.8%Al ALLOY. (SOLUTION TREATED AT 900°C FOR 1 HR.)

Adapted from Brezina (1982)

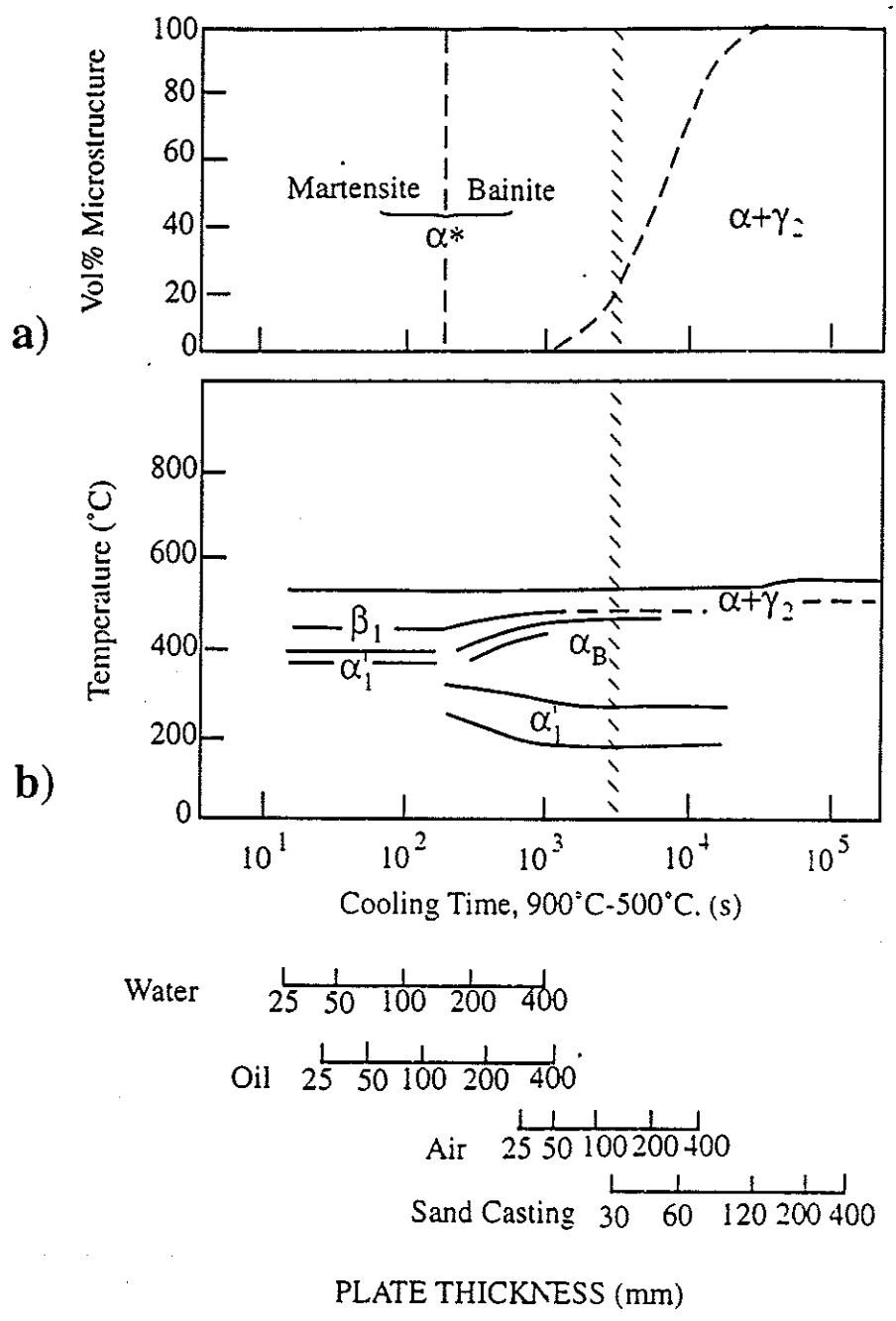

Figure 11. Microstructure map (a) and Continuous-Cooling-Transformation (CCT) Curves (b) for a eutectoidal Cu-Al alloy. Cooling rates and times (experimentally determined) were converted to equivalent bar thicknesses in a given cooling medium, using standard thermal data. Both the map, and the CCT curves relate to the center of the bar. (Adapted from Brezina [1]). The CCT curves and the microstructure maps are both "read" from "top to bottom". Reasonable agreement is seen between the CCT curves of Brezina (this figure) and the TTT curves which were presented in Figure 2. The nomenclature employed is that shown in Tables I and II. Note that α* denotes a mixture of martensite and bainite.

MICROSTRUCTURE MAP AND CCT CURVE FOR A HYPOEUTECTOID Cu-10.5%Al ALLOY. (SOLUTION TREATED AT 850°C FOR 1 HR.)

Adapted from Brezina (1982)

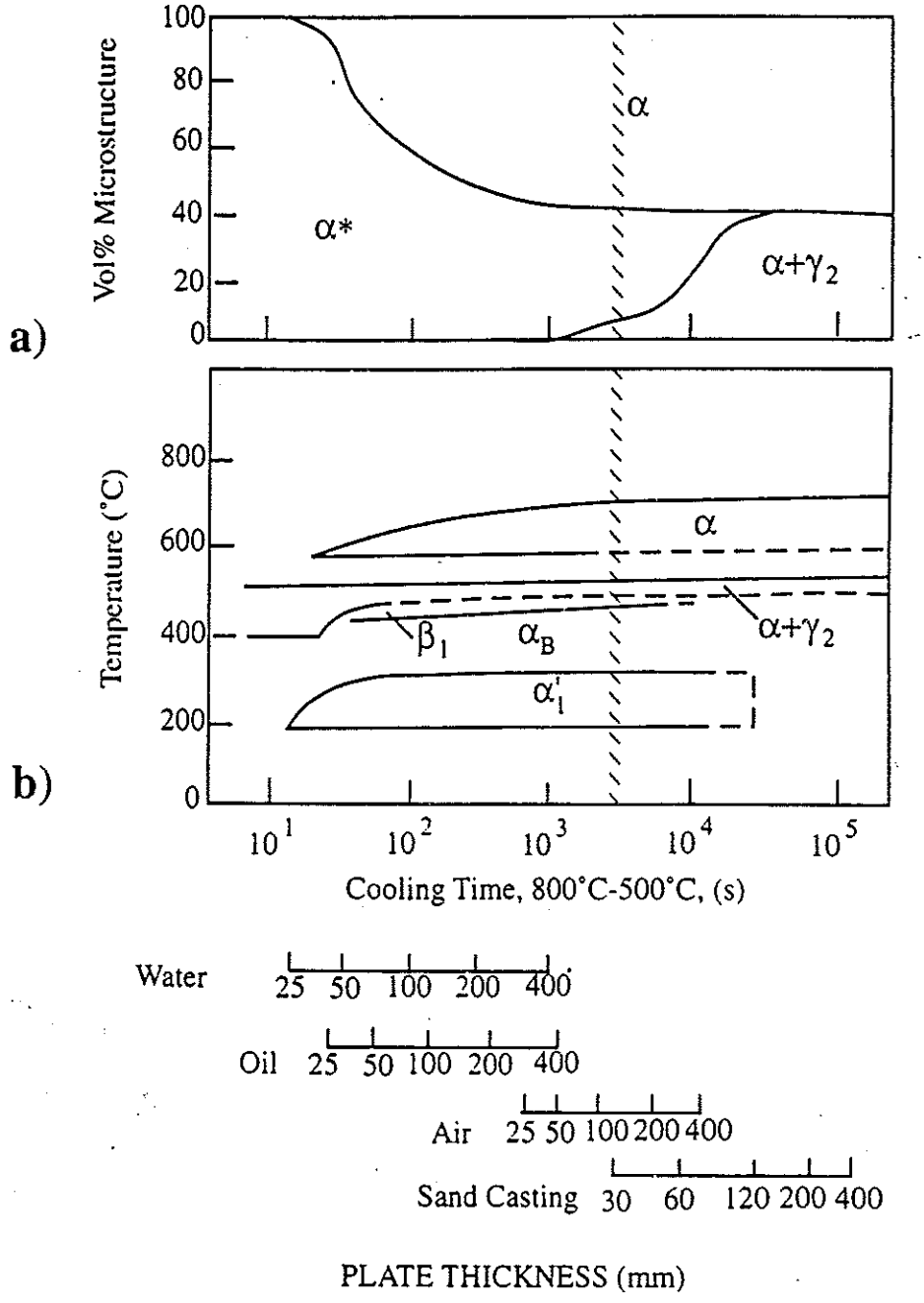

Figure 12. Microstructure map (a) and Continuous-Cooling-Transformation (CCT) Curves (b) for a hypoeutectoid Cu-Al alloy. (Adapted from Brezina [1]). The CCT curves and the microstructure maps are both "read" from "top to bottom". The high temperature "C"-Curve is for the proeutectoid alpha. Note that α* (Figure 12a) denotes a mixture of martensite and bainite

Isothermal Sections of the Cu-Al-Ni, Cu-Al-Fe and Al-Ni-Fe Ternary Phase Diagrams

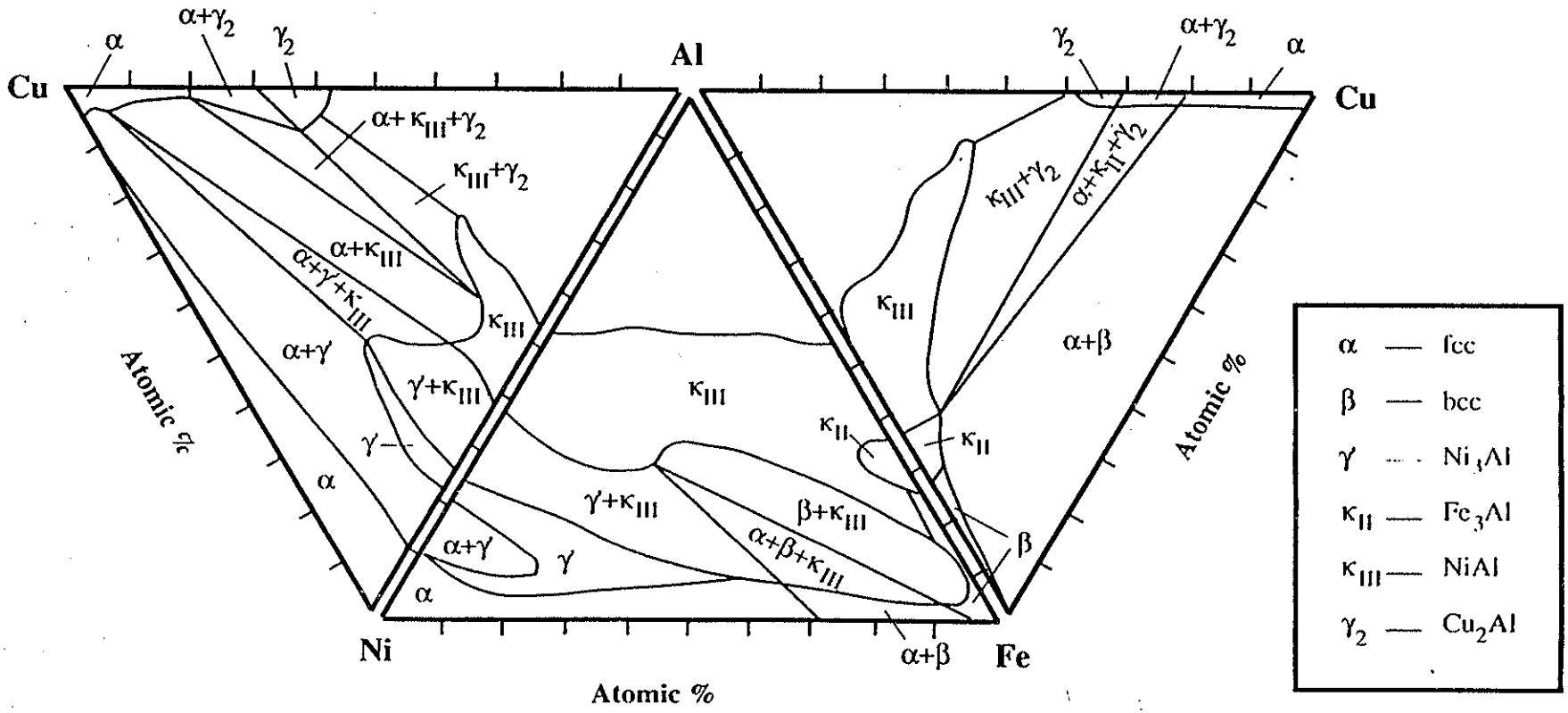

Figure 13. Isothermal sections of the Cu-Al-Ni, Al-Ni-Fe and Cu-Al-Fe ternary phase diagrams showing the phase fields associated with the various intermetallic phases. The figure is adapted from ref.[5], but with a terminology that is consistent with e.g., Tables I and II.

SCHEMATIC MICROSTRUCTURES OF NAB CASTINGS

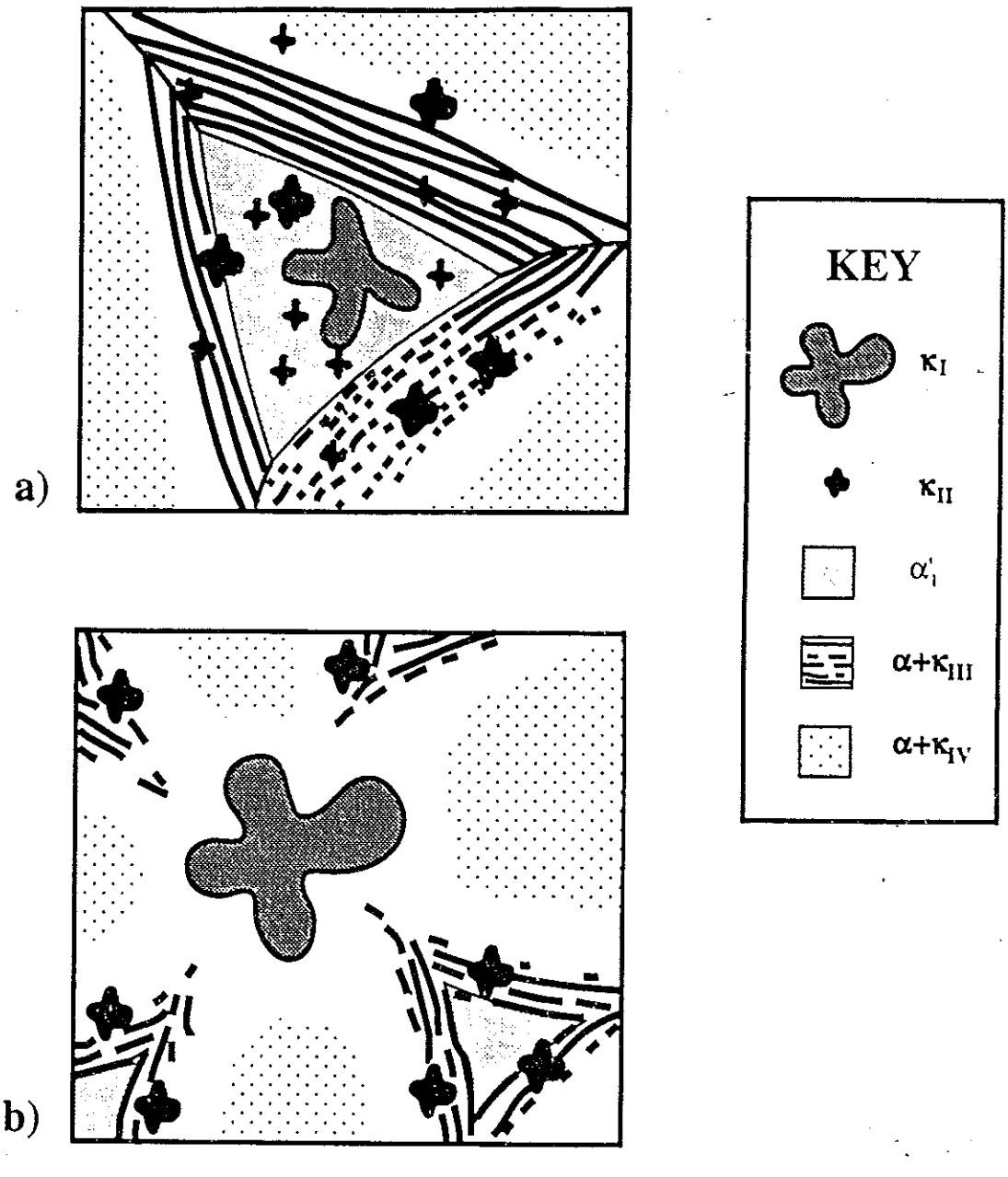

Figure 14. Schematic microstructures developed in slowly cooled, "high-Fe" NAB, according to Brezina [1], Figure 14a; and Lorimer, Ridley and co-workers [9], Figure 14b. Although not explicitely stated, the proeutectoid alpha is rod-like. The encapsulated islands of high-Al martensite are not associated with plates of bainite (and see text).

SCHEMATIC MICROSTRUCTURES OF NAB CASTINGS

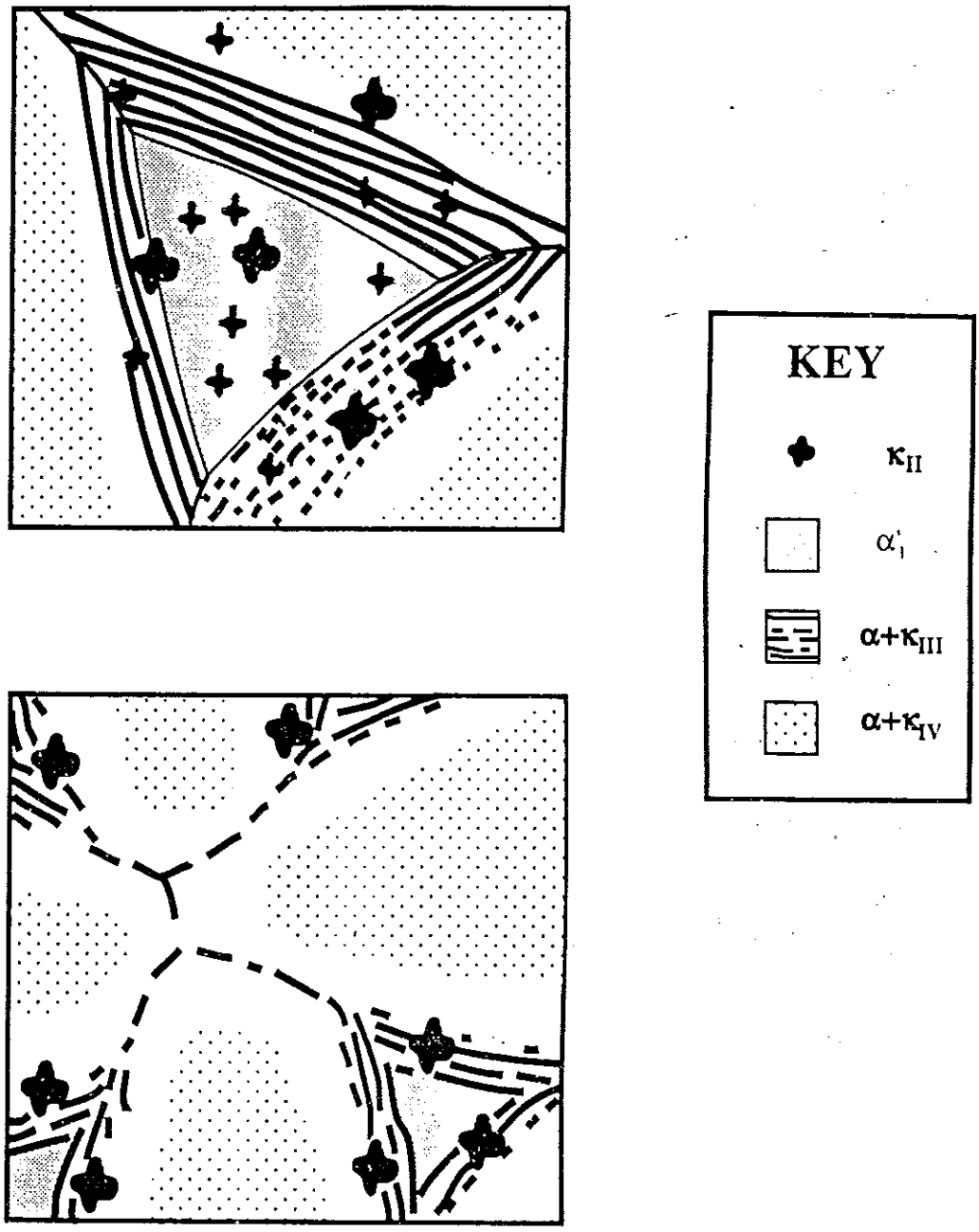

Figure 15. Schematic microstructures developed in slowly cooled, "low-Fe" NAB. The "kappa-one" phase is absent; otherwise, the microstructures are identical to those in Figure 14. (Adapted from refs. [1] and [9])

PROEUTECTOID ALPHA AND THE EUTECTOIDAL MIXTURE OF ALPHA + KAPPA THREE

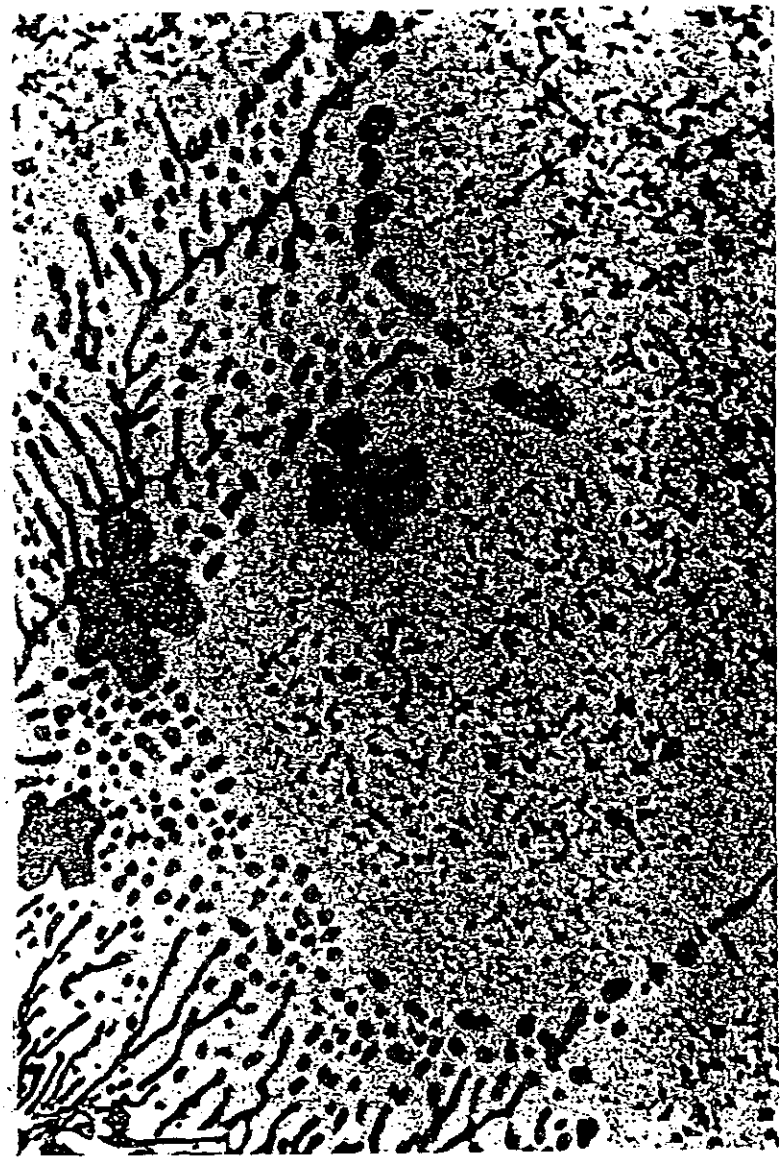

Figure 16a. Light micrograph of slowly cooled NAB. The α contains a dispersion of κ_{IV} precipitates, some of which exhibit a cruciform morphology. Dendritic κ_{II} particles are found, predominantly in the eutectoidal mixture of α + κ_{III} . A κ_{IV} precipitate free zone (PFZ) is present in the vicinity of the eutectoid colonies.

PROEUTECTOID ALPHA, PHASE-SEPARATED KAPPA TWO AND THE EUTECTOIDAL MIXTURE OF ALPHA + KAPPA THREE

Figure 16b. Light micrograph of slowly cooled NAB. The α contains a dispersion of κ_{IV} precipitates, some of which exhibit a cruciform morphology. Dendritic κ_{II} particles are found, predominantly in the eutectoidal mixture of α + κ_{III} . A κ_{IV} precipitate free zone (PFZ) is present in the vicinity of the eutectoid colonies. Note the dissimilar etching characteristics, between the center and the periphery of the κ_{II} particles.

PROEUTECTOID ALPHA, DENDRITIC KAPPA TWO AND HIGH-ALUMINUM MARTENSITE

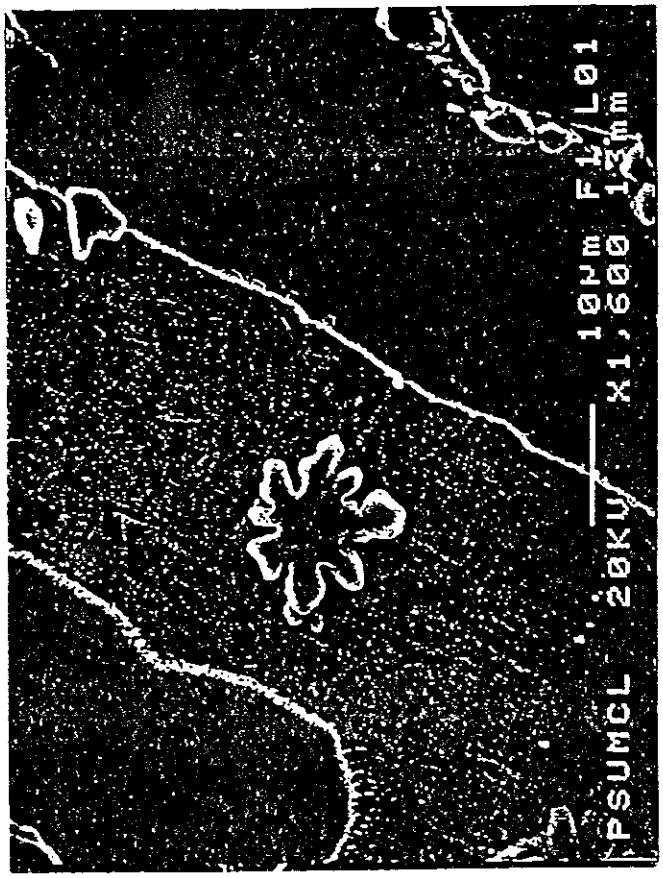

10μm

Figure 17. Scanning electron microscope (SEM) image of a dendritic k_{II} particle in high-aluminum martensite.

RELATIONSHIP BETWEEN THE CRYSTAL STRUCTURES OF THE HIGH TEMPERATURE,DISORDED β PHASE AND THE LOW TEMPERATURE κ PHASES

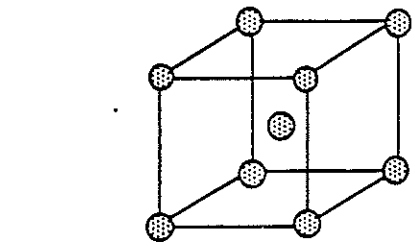

a) β (Disordered bcc)

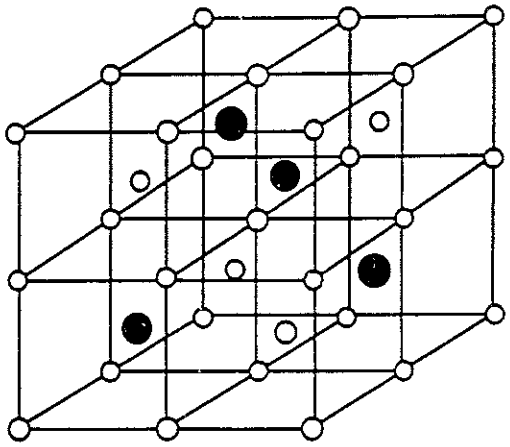

b) $\kappa_{I/II/IV}$ (Single Unit Cell)

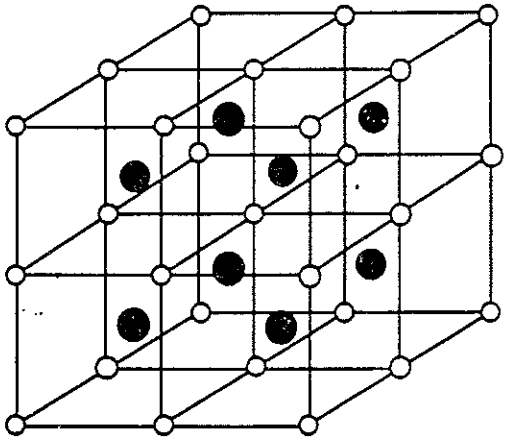

c) κ_{III} (Eight Unit Cells)

Figure 18. Relationship between the crystal structures of the high temperature beta phase and the ordered, intermetallic phases. (Adapted from Hasan et al. [4])
a) The disordered β phase.
b) The Fe_3Al structure of the κ_I , κ_{II} and κ_{IV} phases. The "Fe" positions are occupied by Fe (+ Ni + Cu + Mn). The "Al" positions are occupied by Al (+ Si).
c) The NiAl structure of the κ_{III} phase. The "Ni" positions are occupied by Ni (+ Fe + Cu + Mn). The "Al" positions are occupied by Al (+ Si).

DENDRITIC KAPPA ONE PARTICLES IN ASSOCIATION WITH PROEUTECTOID ALPHA.

Figure 19a. Low magnification light micrograph of slowly cooled NAB. The microstructure contains "clusters" of κ_I particles in association with of rods of proeutectoid α.

DENDRITIC KAPPA ONE PARTICLES IN ASSOCIATION WITH PROEUTECTOID ALPHA.

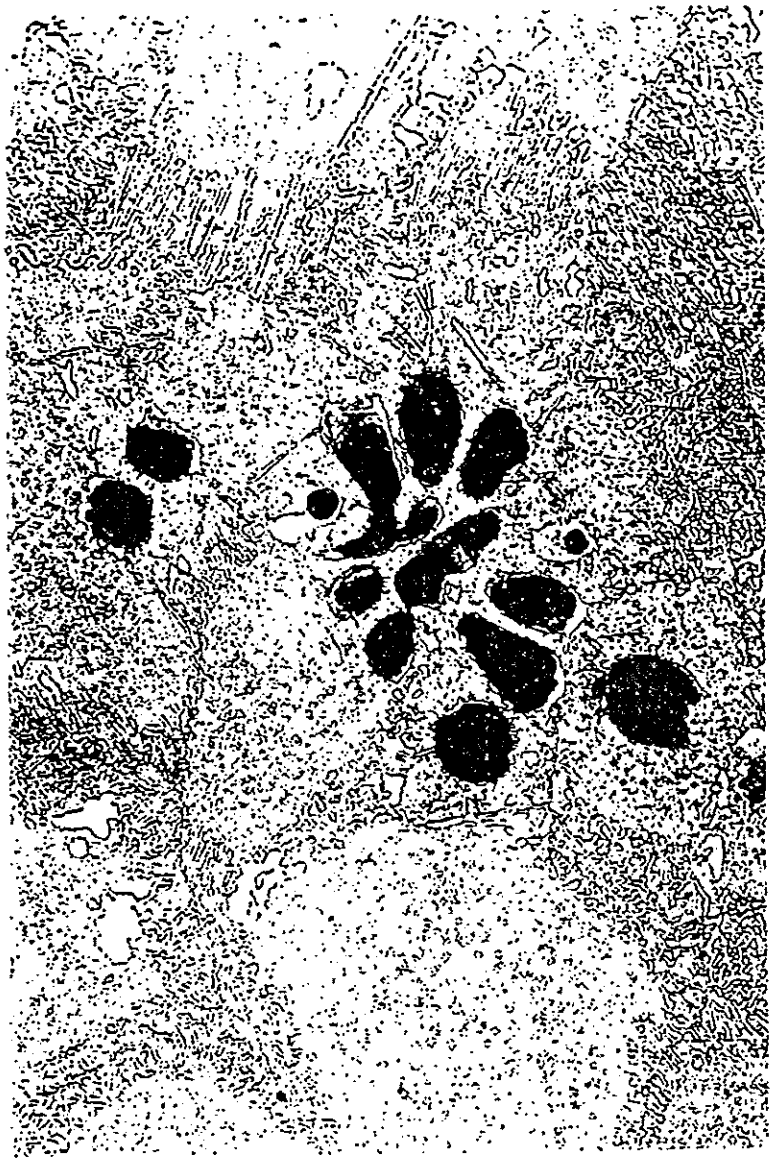

Figure 19b. Higher magnification light micrograph of slowly cooled NAB (same region as Figure 19a). The microstructure contains a cluster of κ_I particles.

CRUCIFORM "KAPPA-FOUR" PRECIPITATES

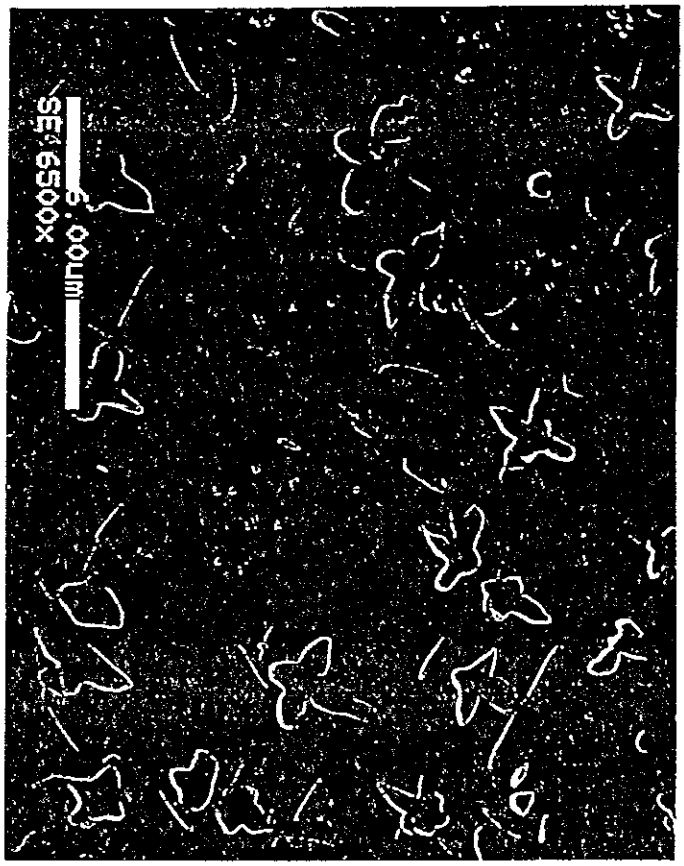

Figure 20. Scanning electron microscope (SEM) image of cruciform κ_{IV} particles in proeutectoid alpha.

KAPPA THREE PARTICLES IN ASSOCIATION WITH PROEUTECTOID ALPHA.

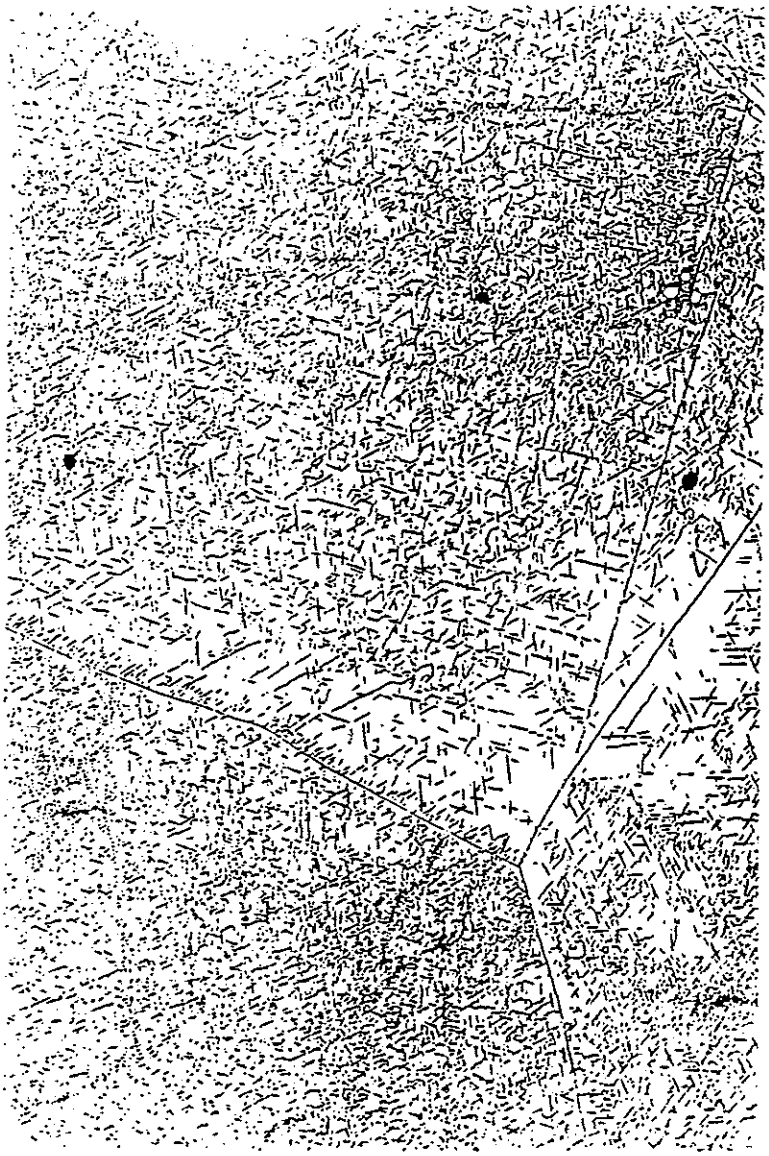

Figure 21. Light micrograph of a tempered NAB. The proeutectoid α grains contain a dispersion of κ_{III}.

VERTICAL SECTION OF THE Cu-Al-5%Ni-5%Fe PHASE DIAGRAM

Adapted from Cook et al. (1951-1952)

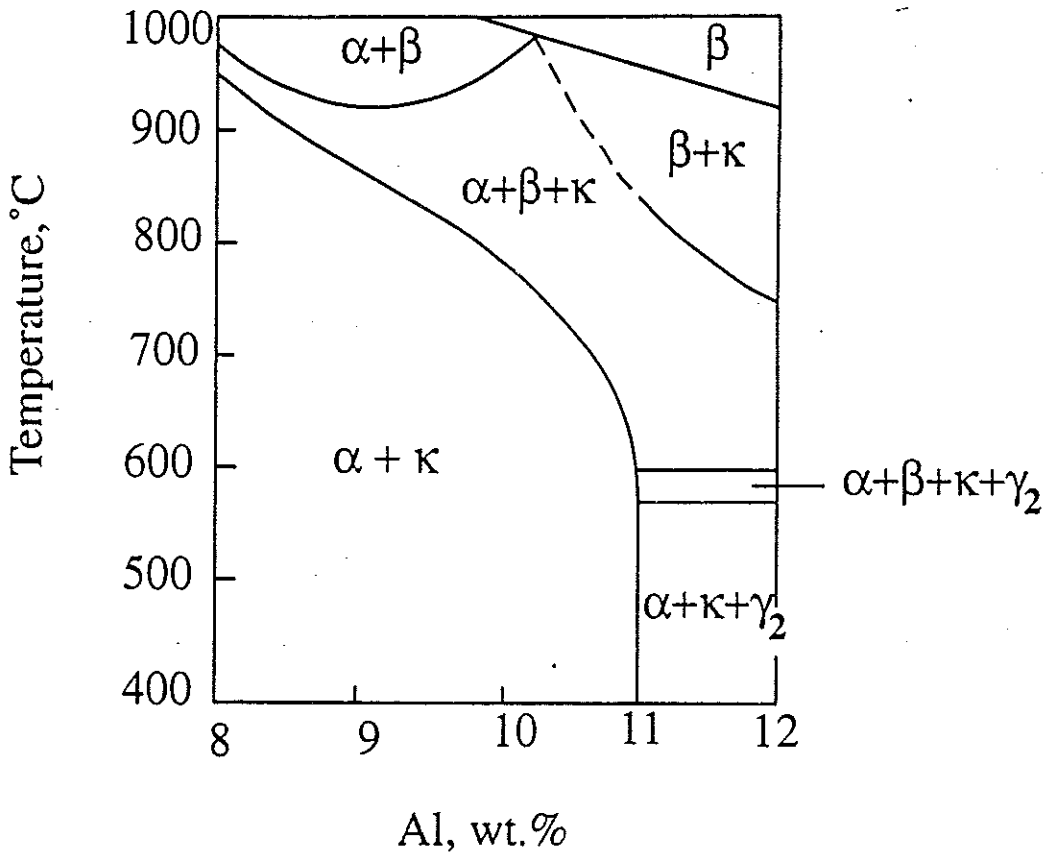

Figure 22. Vertical section of the Cu-Al-5%Ni-5%Fe phase diagram. (Adapted from Cook, Fentiman and Davis [13]). No distinction between κ_{II} and κ_{III} has been attempted.

COMPOSITION/TEMPERATURE/MICROSTRUCTURE MAP
(Cook et al., 1951-1952)

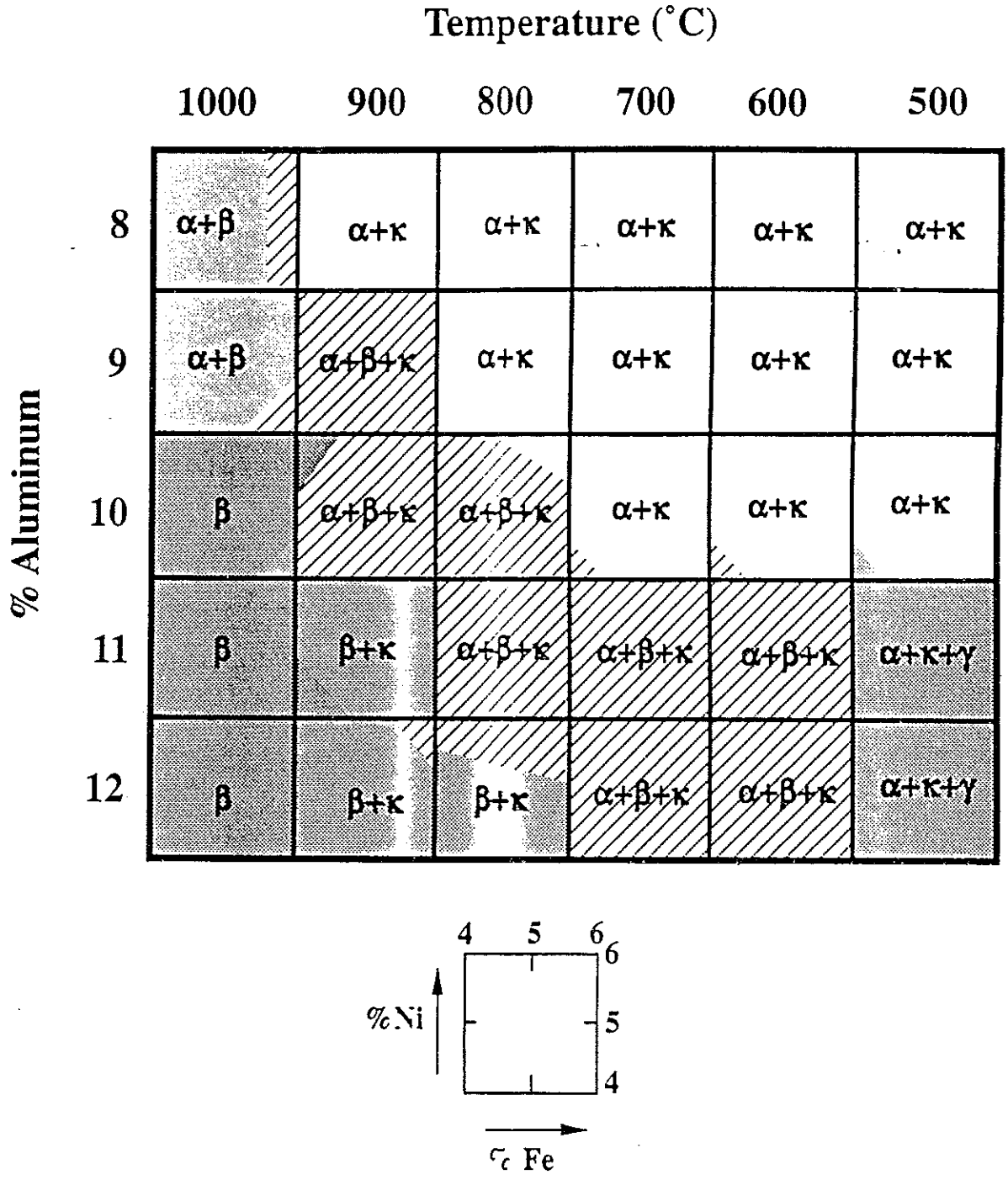

Figure 23. Composition/Temperature/Microstructure Maps for a series of nickel-aluminum bronzes. Each square represents a microstructure map, at constant temperature and aluminum levels, for nickel and iron contents between four and six percent. The centers of each square correspond to a composition of Cu-x%Al-5%Fe-5%Ni. (Adapted from Cook, Fentiman and Davis [13]).

VERTICAL SECTION OF THE Cu-Al-5%Ni-5%Fe PHASE DIAGRAM

Adapted from Brezina (1982)

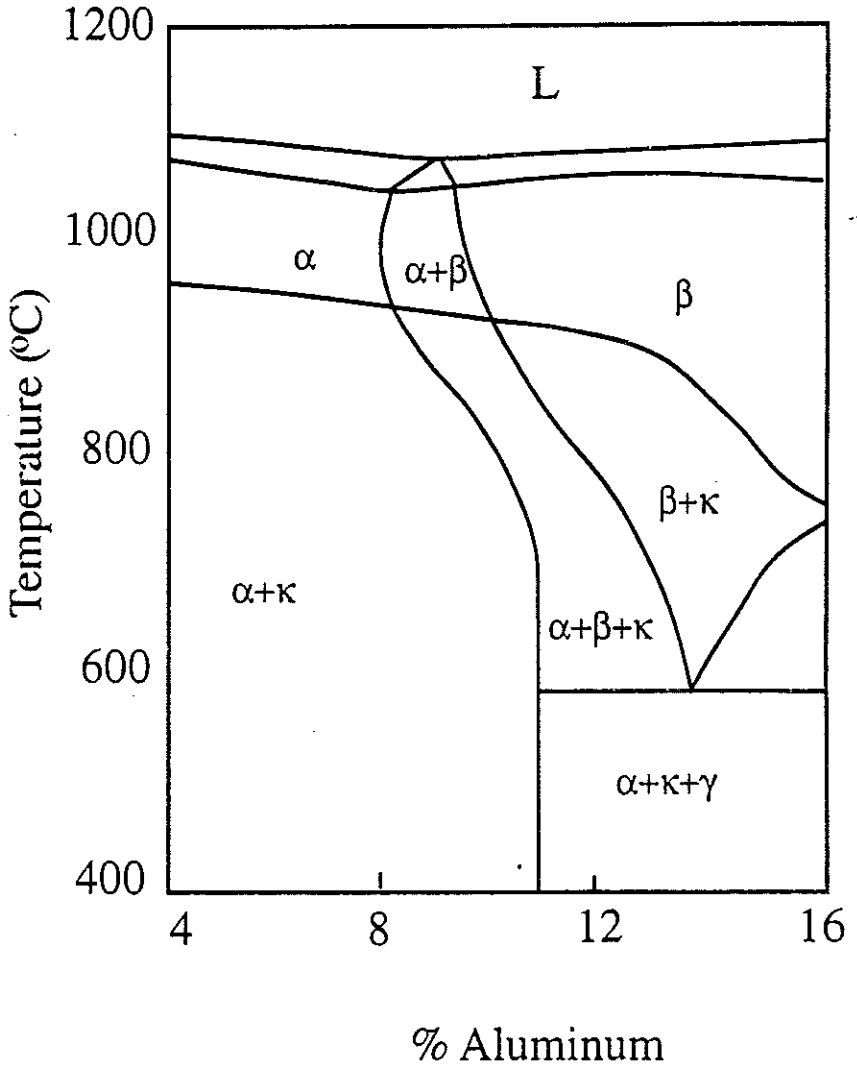

Figure 24. Vertical section through the Cu-Al-5%Ni-5%Fe phase diagram. (Adapted from Brezina [1]). There is very little substantive difference between this diagram and that previously presented by Cook et al., [13}, and see Figure 22.

VERTICAL SECTION OF THE Cu-Al-5%Ni-5%Fe PHASE DIAGRAM

Adapted and Emended from Cook et al. (1951-1952)

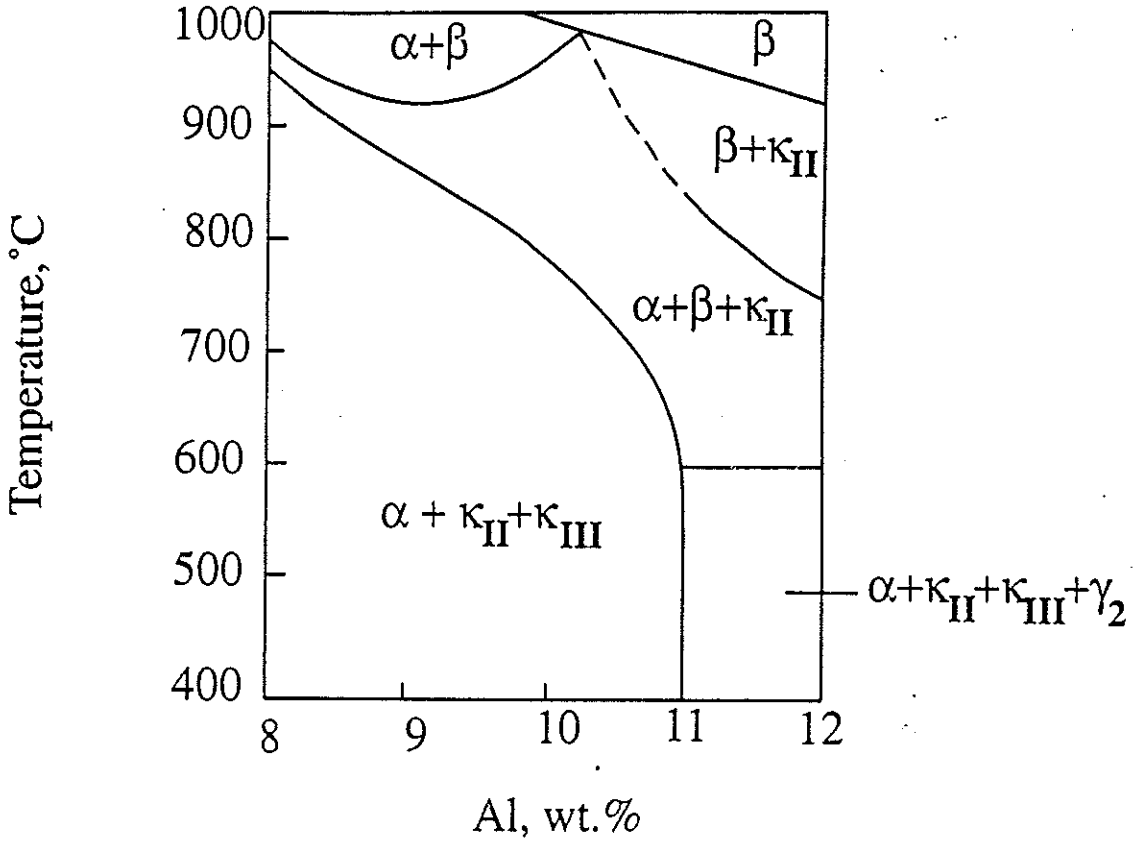

Figure 25. Proposed vertical section of the Cu-Al-5%Ni-5%Fe phase diagram. The diagram retains the solvus lines of Cook et al., [13], but with a terminology which is based on that detailed in Tables I and II. (Adapted and Emended from ref.[13])

TRANSFORMATIONS FROM THE HIGH TEMPERATURE BETA PHASE DURING SLOW COOLING.

Emended from Culpan and Rose [16]

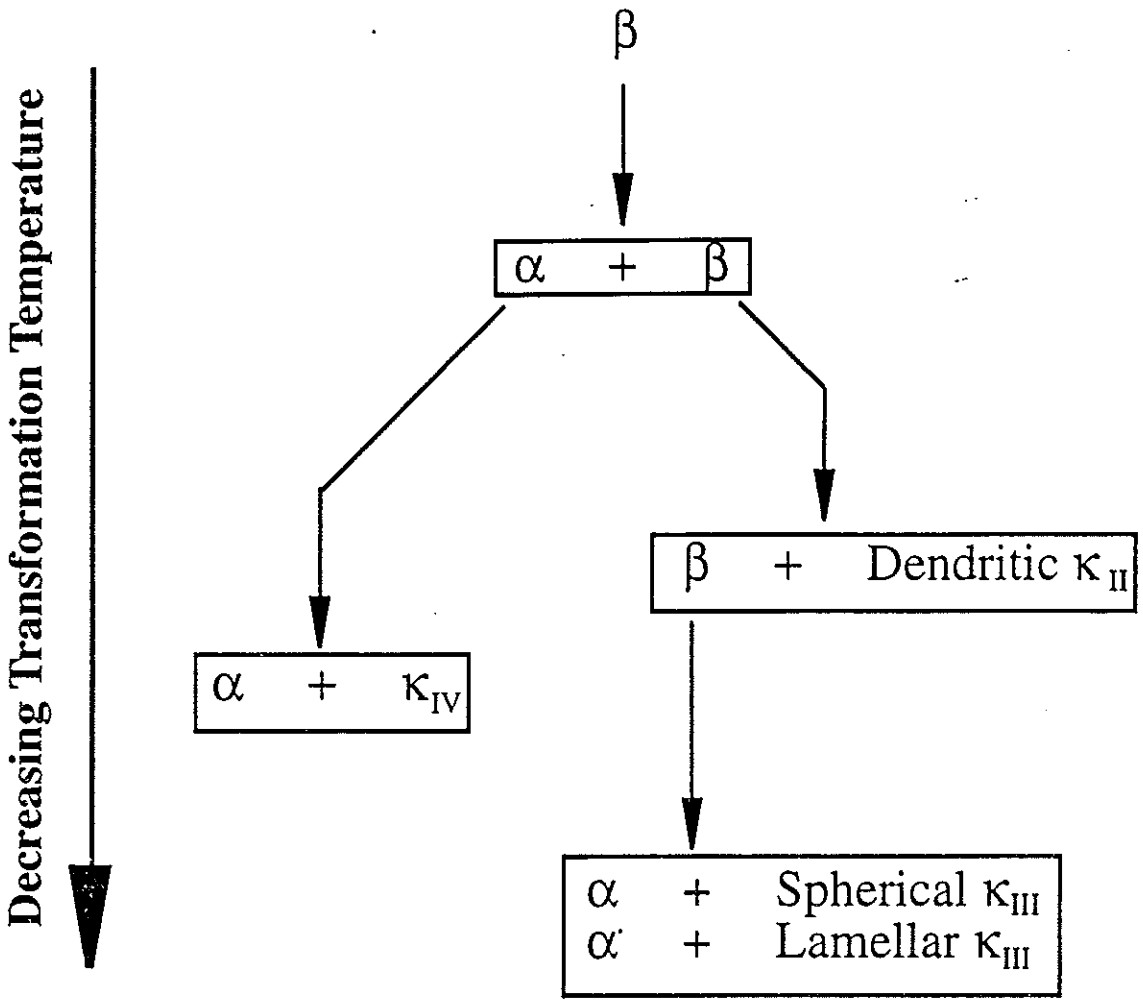

Figure 26. Schematic diagram of the transformations that *can* occur during slow cooling of NAB from the beta range. The nomenclature adopted is consistent with that shown in Tables I and II. It is assumed that the beta is fully transformed, by diffusional mechanisms, to a mixture of alpha plus kappa phases: neither bainite nor martensite is formed. (Emended from Culpan and Rose [16])

MICROSTRUCTURE MAP AND CCT CURVE FOR A Cu-8.8%Al-5.4%Fe-5%Ni-0.9%Mn ALLOY. (SOLUTION TREATED AT 950°C FOR 1 HR.)

Adapted from Brezina (1982)

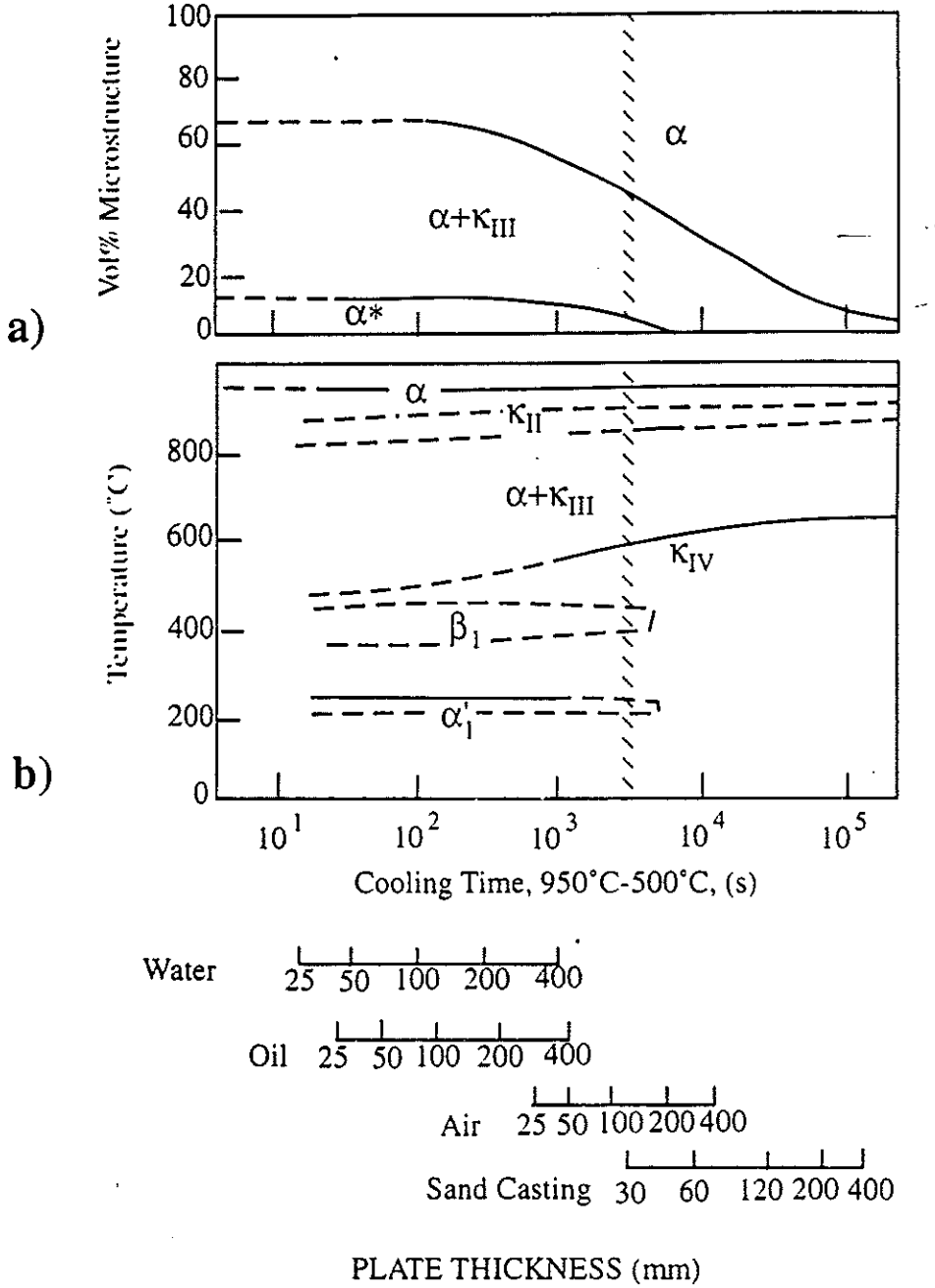

Figure 27. Microstructure map (a) and Continuous-Cooling-Transformation (CCT) Curves (b) for a Nickel-Aluminum Bronze (NAB). The CCT curves and the microstructure maps are both "read" from "top to bottom". (Adapted from Brezina [1]). There are three high tempertature "C"-Curves; for the proeutectoid alpha, the dendritic kappa two and the eutectoid mixture. Note that α* (Figure 27a) denotes a mixture of martensite and bainite.

MICROSTRUCTURE MAP AND CCT CURVE FOR A Cu-9.9%Al-5.3%Fe-5.1%Ni-0.9%Mn ALLOY. (SOLUTION TREATED AT 950°C FOR 1 HR.)

Adapted from Brezina (1982)

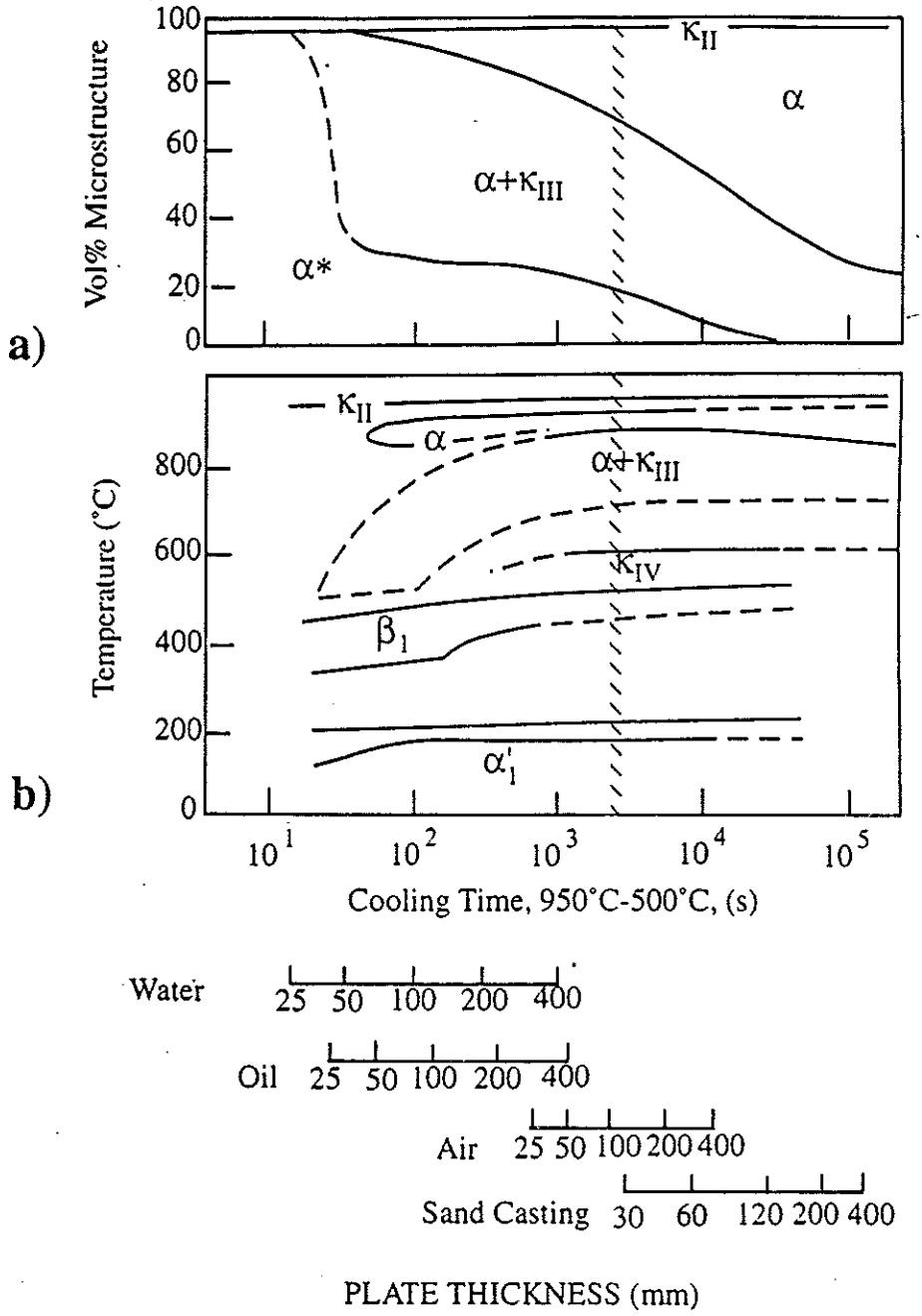

Figure 28. Microstructure map (a) and Continuous-Cooling-Transformation (CCT) Curve (b) for a Nickel-Aluminum Bronze (NAB). (Adapted from Brezina [1]). The CCT curves and the microstructure maps both indicate that this higher aluminum-containing alloy has a higher hardenability than the alloy shown in Figure 27. Hence, it would be easier to form martensite in this alloy, as compared with the 8.8% Al alloy.

ARRET REFROIDISSANT (Ar) TEMPERATURES, AND SOLUTION TREATMENT TEMPERATURES FOR A NICKEL-ALUMINUM BRONZE

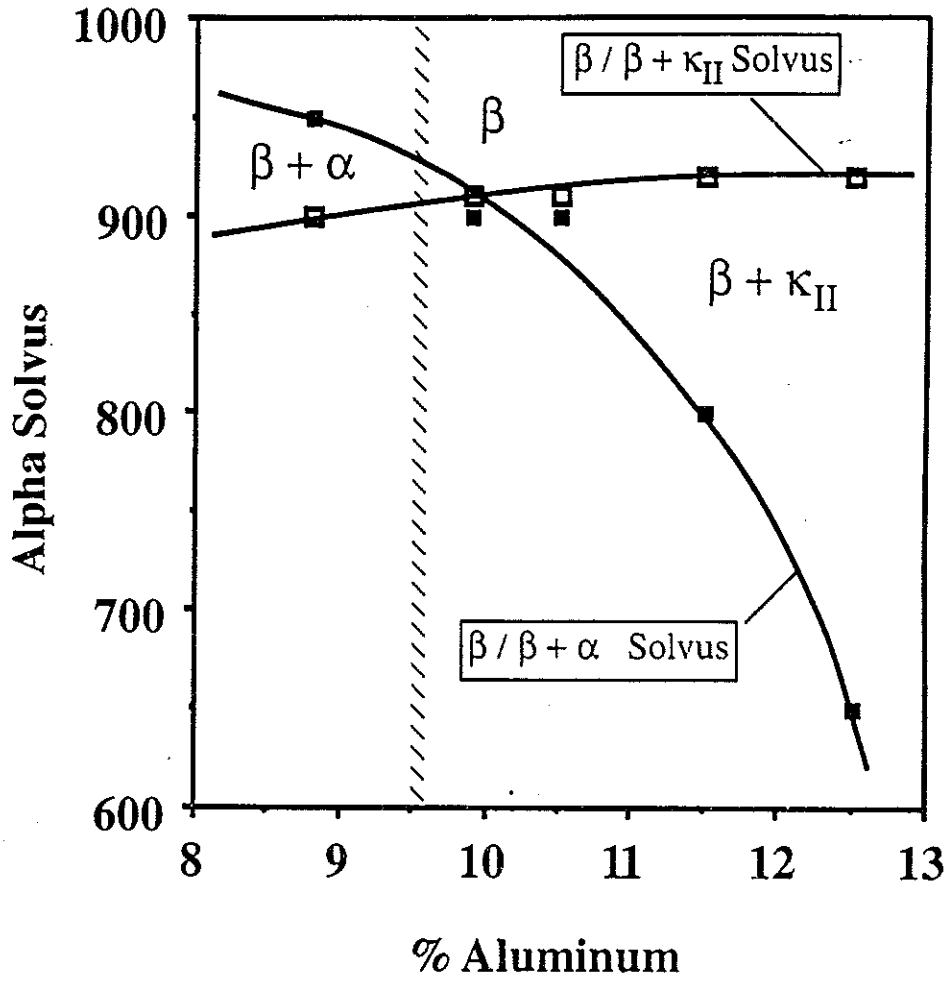

Figure 29a. The arret refroidissant (Ar) temperatures for Cu-Al-5%Ni-5%Fe alloys. These curves can be used to estimate the lowest temperatures for full solution treatment (*supercritical annealing*). A 9.5% aluminum bronze would require a temperature somewhat in excess of 930°C. (Data abstracted from Brezina [1])

DEFINITION OF *SUBCRITICAL, INTERCRITICAL* AND *SUPERCRITICAL* ANNEALING.

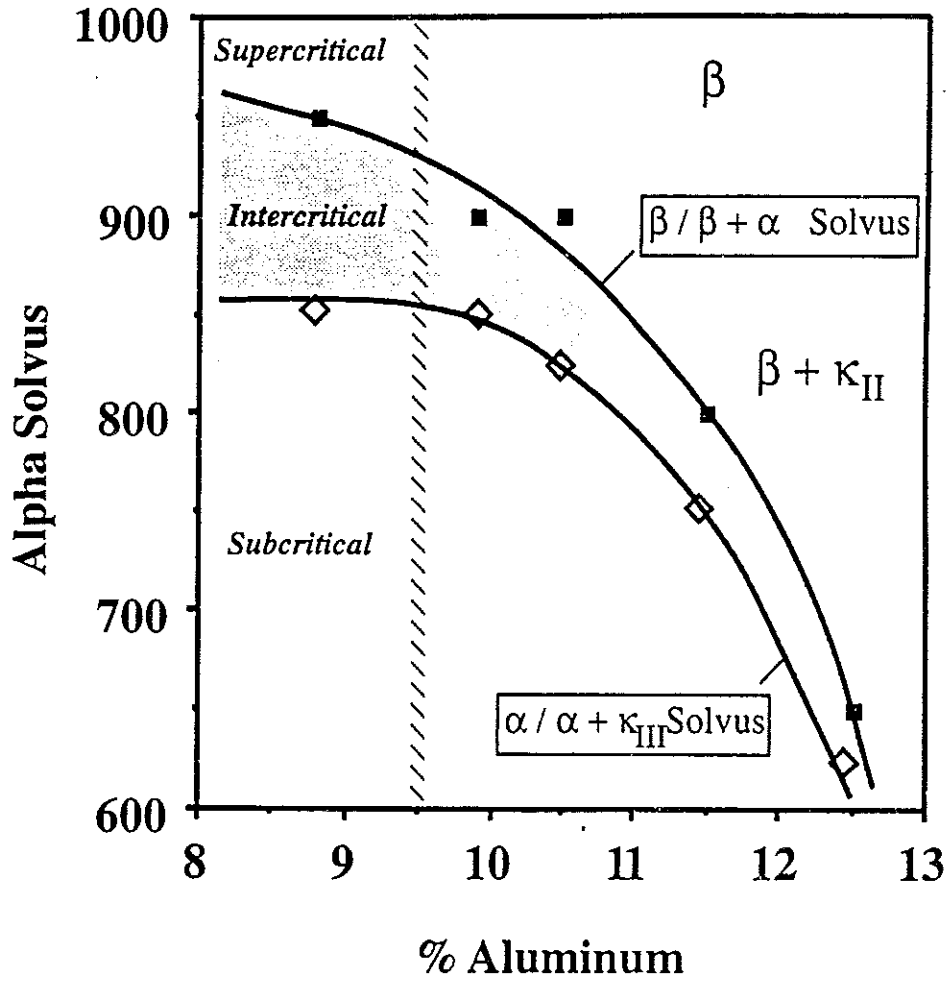

Figure 29b. Subcritical, intercritical and supercritical annealing of a 9.5% Al, NAB. A subcritical anneal is equivalent to a tempering treatment: a supercritical anneal to a solution treatment.

PERCENTAGE EUTECTOID MICROCONSTITUENT AS A FUNCTION OF ALUMINUM CONTENT FOR SLOW COOLING.

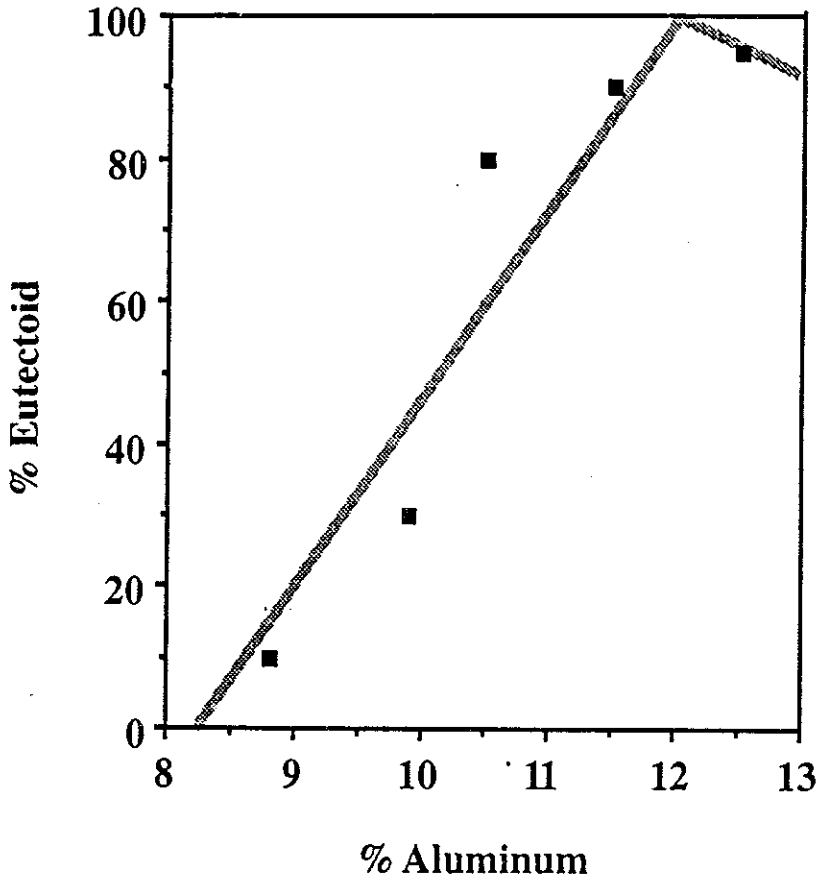

Figure 30. Percentage of the eutectoid microconstituent as a function of the aluminum content. (Data abstracted from the CCT and μmaps of Brezina [1], and for sand castings of 200mm thick plate). The first four datum points relate to hypoeutectoid alloys, whereas the 12.5% Al alloy is hypereutectoid. The 11.5% and 12.5% alloys contain both the $\alpha + \kappa$ and $\alpha + \gamma$ eutectoid products. The data also suggest that alloys with less than ~8%Al will contain little or no $\alpha + \kappa$ eutectoid.

KAPPA THREE PARTICLES IN ASSOCIATION WITH PROEUTECTOID ALPHA GRAIN BOUNDARIES IN A LOW-Al NAB.

Figure 31. Light micrograph of a slowly cooled, low-aluminum NAB. No eutectoidal mixture is observed. However, there is a large number density of κ_{III} particles at the grain boundaries.

SCHEMATIC MICROSTRUCTURE MAP FOR A Cu-9.5%Al-5%Fe-5%Ni ALLOY.

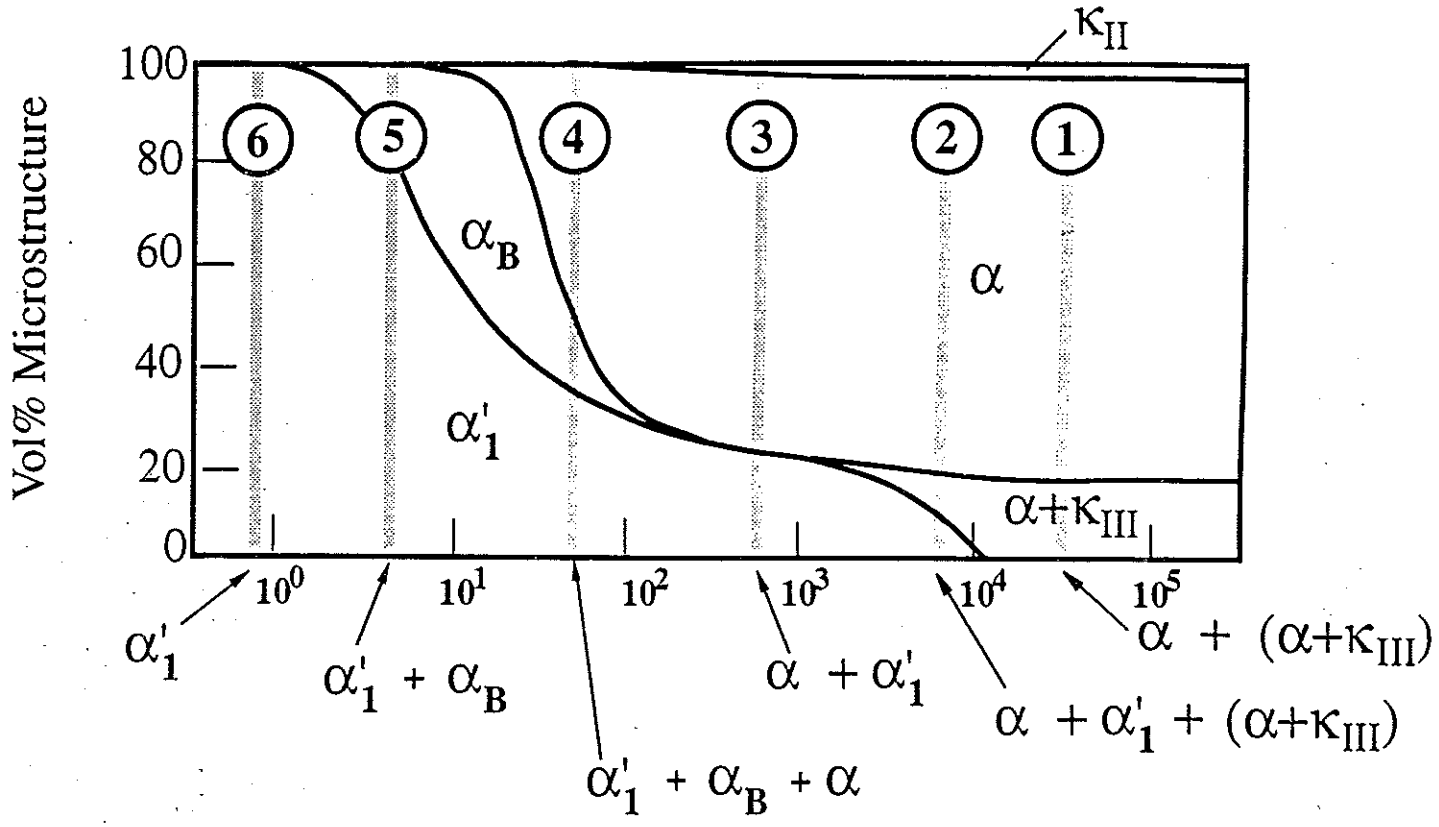

Figure 32. Hypothetical microstructure map for NAB, showing a complete range of transformation products from martensite (α'_1) at the highest cooling rate (6), to the equilibrium volume fraction of proeutectoid α plus the eutectoid mixture of $\alpha + \kappa_{III}$ at slow cooling rates (1). In "theory", six "unique" microstructures can be obtained by continuous cooling alone, these being:

(1) Proeutectoid Alpha + Eutectoid
(2) Proeutectoid Alpha + Eutectoid + Martensite.
(3) Proeutectoid Alpha + Martensite
(4) Proeutectoid Alpha + Martensite + Bainite.
(5) Martensite + Bainite.
(6) 100% Martensite.

In practice, however, it is not feasible to produce 100% Martensite

PROEUTECTOID ALPHA AND HIGH-ALUMINUM MARTENSITE IN A NAB WELD.

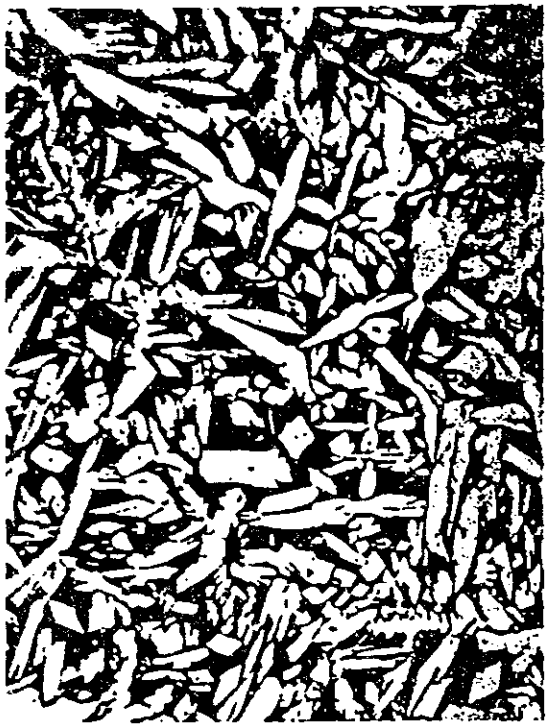

Figure 33. Light micrograph of proeutectoid α and high-aluminum martensite in a weld.

PROEUTECTOID ALPHA AND HIGH-ALUMINUM MARTENSITE IN AN INTERCRITICALLY ANNEALED NAB

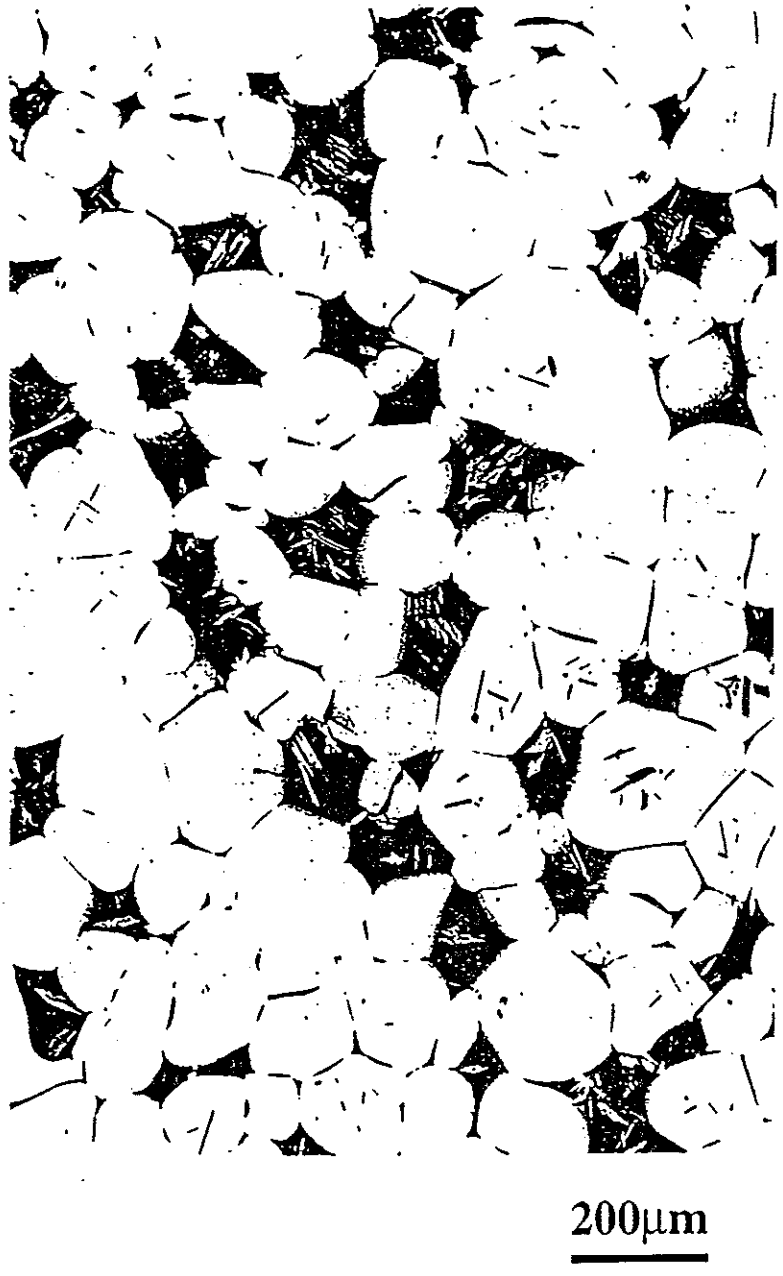

Figure 34. Light micrograph of proeutectoid α and high-aluminum martensite in material which had been intercritically annealed and subsequently oil-quenched.

PROEUTECTOID ALPHA, BAINITE AND HIGH-ALUMINUM MARTENSITE IN AN INTERCRITICALLY ANNEALED NAB

Figure 35. Light micrograph of proeutectoid α, bainite and high-aluminum martensite in material which had been intercritically annealed and subsequently air-quenched.